© 2020. Published by The Company of Biologists Ltd | Development (2020) 147, dev186130. doi:10.1242/dev.186130

RESEARCH ARTICLE

Specification and regulation of vascular tissue identity in the *Arabidopsis* embryo

Margot E. Smit[1,*], Cristina I. Llavata-Peris[1,‡], Mark Roosjen[1], Henriette van Beijnum[1,§], Daria Novikova[1,2,3], Victor Levitsky[2,3], Iris Sevilem[4], Pawel Roszak[4,5], Daniel Slane[6], Gerd Jürgens[6], Victoria Mironova[2,3], Siobhan M. Brady[7] and Dolf Weijers[1,¶]

ABSTRACT

Development of plant vascular tissues involves tissue identity specification, growth, pattern formation and cell-type differentiation. Although later developmental steps are understood in some detail, it is still largely unknown how the tissue is initially specified. We used the early *Arabidopsis* embryo as a simple model to study this process. Using a large collection of marker genes, we found that vascular identity was specified in the 16-cell embryo. After a transient precursor state, however, there was no persistent uniform tissue identity. Auxin is intimately connected to vascular tissue development. We found that, although an AUXIN RESPONSE FACTOR5/MONOPTEROS (ARF5/MP)-dependent auxin response was required, it was not sufficient for tissue specification. We therefore used a large-scale enhanced yeast one-hybrid assay to identify potential regulators of vascular identity. Network and functional analysis of candidate regulators suggest that vascular identity is under robust, complex control. We found that one candidate regulator, the G-class bZIP transcription factor GBF2, can modulate vascular gene expression by tuning MP output through direct interaction. Our work uncovers components of a gene regulatory network that controls the initial specification of vascular tissue identity.

KEY WORDS: *Arabidopsis*, Vascular development, Auxin, Embryo, Gene regulatory network

INTRODUCTION

Vascular tissues play a central role in plant growth and development by providing plants with transport capabilities and structural support. The various steps of vascular tissue development have been studied in some detail, mainly in the *Arabidopsis* leaf (Donner et al., 2009; Gardiner et al., 2011; Krogan et al., 2012), shoot (Etchells et al., 2013; Hirakawa et al., 2010; Smetana et al., 2019; McConnell et al., 2001; Han et al., 2018) and root (Scheres et al., 1995; Miyashima et al., 2019; De Rybel et al., 2014). From this wealth of studies, a picture emerges in which dedicated regulatory modules function to create a properly sized and patterned transport bundle. Several steps can be recognized in this process: specification of vascular tissue identity, cell proliferation to generate a bundle of cells, patterning into xylem, phloem and cambium cell types, and finally differentiation into functional transport cells. The regulators and effectors of all but the first step have been dissected in some detail.

The rate of proliferation by periclinal cell divisions determines the width of a vascular bundle. Periclinal cell divisions in the vascular cells are controlled by several pathways: one directed by the xylem-expressed TARGET OF MONOPTEROS 5 (TMO5)/LONESOME HIGHWAY (LHW) dimer (De Rybel et al., 2013, 2014; Ohashi-Ito et al., 2014, 2013), another regulated by the phloem-expressed PHLOEM EARLY DOFs (PEARs) (Miyashima et al., 2019) and a third depending on the activity of WUSCHEL-LIKE HOMEOBOX 4 and 14 in the cambium (WOX4/14) (Etchells et al., 2013; Fisher and Turner, 2007; Hirakawa et al., 2010; Smit et al., 2020). In concert with proliferation, cells in the vascular bundle develop a pattern of distinct sub-identities. Xylem development is associated with high auxin signaling, and further specification of protoxylem or metaxylem identity depends on a combination of the cytokinin response and the activity of HD-ZIP III transcription factors (Baima et al., 2001; Bishopp et al., 2011; Carlsbecker et al., 2010; Mähönen et al., 2006; McConnell et al., 2001). Conversely, the specification of phloem identity is associated with high cytokinin activity and the presence of, among others, ALTERED PHLOEM DEVELOPMENT (APL) (Bonke et al., 2003). Located between the phloem and xylem, the meristem-like (pro)cambium has been shown to contribute to both the xylem and the phloem cell populations (Smetana et al., 2019).

Finally, several vascular cell types undergo irreversible terminal differentiation. The differentiation of xylem vessel elements can be triggered when a gene regulatory network under the control of VASCULAR-RELATED NAC-DOMAIN6 (VND6) and VND7 is initiated (Kubo et al., 2005; Yamaguchi et al., 2010; McCarthy et al., 2009). Although no differentiation-inducing factor has yet been found to trigger phloem-like differentiation (Blob et al., 2018), several factors necessary for phloem differentiation have been identified (Ruiz Sola et al., 2017; Rodriguez-Villalon et al., 2014; Wallner et al., 2017).

Most of the studied regulators of vascular development are expressed only, or preferentially, in vascular cells, which suggests the existence of a robust genetic identity. However, how this vascular tissue identity is initially specified has so far remained

[1]Laboratory of Biochemistry, Wageningen University, Stippeneng 4, Wageningen, 6708WE, The Netherlands. [2]Novosibirsk State University, LCT&EB, Novosibirsk, 630090, Russia. [3]Institute of Cytology and Genetics, Novosibirsk, 630090, Russia. [4]Institute of Biotechnology, HiLIFE/Organismal and Evolutionary Biology Research Programma, Faculty of Biological and Environmental Sciences, Viikki Plant Science Centre, University of Helsinki, Helsinki, 00014, Finland. [5]Sainsbury Laboratory, University of Cambridge, Cambridge, CB2 1LR, UK. [6]Max Planck Institute for Developmental Biology, Cell Biology, Tübingen, 72076, Germany. [7]Department of Plant Biology and Genome Center, University of California Davis, Davis, CA 95616, USA.
*Present address: Howard Hughes Medical Institute/Department of Biology, Stanford University, Stanford, CA 94305-5020, USA. ‡Present address: Laboratory of Virology, Wageningen University, Droevendaalsesteeg 1, 6708PB Wageningen, The Netherlands. §Present address: Hubrecht Institute for Developmental Biology and Stem Cell Research, Utrecht, The Netherlands.

¶Author for correspondence (dolf.weijers@wur.nl)

M.E.S., 0000-0001-8285-5130; C.I.L.-P., 0000-0002-0986-2219; P.R., 0000-0002-7822-494X; G.J., 0000-0003-4666-8308; V.M., 0000-0003-3438-0147; S.M.B., 0000-0001-9424-8055; D.W., 0000-0003-4378-141X

Handling Editor: Ykä Helariutta
Received 6 November 2019; Accepted 5 March 2020

Development (2020) 147, dev186130. doi:10.1242/dev.186130

elusive. *De novo* vascular identity specification occurs repeatedly during the plant life cycle as new organs develop or when tissues are wounded (León et al., 2001; Melnyk et al., 2015; Yin et al., 2012). Specification of tissue identities involves the local accumulation of a signaling molecule (small molecule, peptide or protein) that will either promote or suppress the activation of a cell type-specific gene regulatory network. Such mechanisms have been described in non-hair versus hair cells in the root (Lee and Schiefelbein, 1999; Bernhardt et al., 2005), in meristemoids versus stomatal-lineage ground cells in the stomatal lineage (Zhang et al., 2016; Yang et al., 2015; Lau et al., 2014) and in xylem versus phloem cells in the vascular bundle (Smetana et al., 2019; Mähönen et al., 2000; Baima et al., 2001).

A signaling molecule that is strongly correlated with vascular development is auxin. Vascular tissue formation can be triggered by treatments with auxin (Sachs, 1981; Wetmore and Rier, 1963) and, as a result, auxin maxima are often associated with vascular development (Brackmann et al., 2018; Mattsson et al., 2003; Miyashima et al., 2019; Scarpella et al., 2006; Wabnik et al., 2013). Conversely, lack of the AUXIN RESPONSE FACTOR5/MONOPTEROS (ARF5/MP) transcription factor causes impaired vascular development in the *Arabidopsis* embryo, seedling, leaf and stem (Berleth and Jürgens, 1993; Hamann et al., 1999; Hardtke and Berleth, 1998; Mayer et al., 1991; Przemeck et al., 1996). Indeed, MP controls a variety of vascular-specific genes and pathways (De Rybel et al., 2013; Donner et al., 2009; Möller et al., 2017; Schlereth et al., 2010; Yoshida et al., 2019). However, all reported perturbations of auxin activity (synthesis, transport and response) that affect vascular development also affect a range of other processes (Bennett et al., 1996; Cheng et al., 2006; Marchant, 1999; van den Berg and ten Tusscher, 2017). It is therefore difficult to separate a role for auxin in the specification of vascular identity from its many other functions, which warrants the use of a simple developmental model system for studying initial vascular tissue specification in the absence of a certain process, such as differentiation. The early embryo is an attractive model given that it lacks a confounding wound response or extensive proliferation. Its simplicity and predictable division pattern allow the detection of early developmental defects (Scheres et al., 1994), and available transcriptome resources (Palovaara et al., 2017; Belmonte et al., 2013; Schon and Nodine, 2017; Slane et al., 2014) enable in-depth investigations of vascular identity specification.

Here, we first use a suite of established and novel transcriptional reporters to track the stepwise specification of vascular tissue identity in the embryo. We find that the identity initially specified is unique to the embryo, transitioning to a mature and robust identity in the root. We show that auxin response is necessary but not sufficient to specify vascular identity. Via large-scale enhanced yeast one-hybrid (eY1H) assays, we identify common regulators of vascular genes, and we find that one of these, the bZIP transcription factor GBF2, can interact with ARFs and modifies ARF5/MP activity in the regulation of vascular-specific genes.

RESULTS

Specification of vascular tissue identity is a multi-step process

As cell-type identity is often specified at the level of gene activity, it can be inferred using gene expression markers. Each gene expression marker acts as a proxy for an aspect of cell identity and cells that express multiple markers can confidently be identified as having the corresponding identity. We operationally define markers as positively or negatively marking a cell type, but should note that the true absence of marker expression is difficult to show or prove, and is perhaps not biologically realistic. Therefore, we address expression patterns, as well as relative expression strength across cells, to help define markers and cell types. Here, we used a large and diverse set of established cell type markers to ask when vascular tissue specification occurs during embryogenesis and to determine the ontogeny of the tissue. We selected *SHORTROOT* (*SHR*) and *ATHB8* as early vascular markers in root and leaf development (Baima et al., 2001; Gardiner et al., 2011; Long et al., 2015). *ZWILLE* (*ZLL*) shows vascular-specific expression in the root and embryo (Radoeva et al., 2016; Tucker et al., 2008; Haseloff, 1999). *WOODEN LEG* (*WOL*), *PEAR1* and *DOF6* are all associated with cytokinin-responsive growth in the vascular bundle of the root (Mähönen et al., 2000; Miyashima et al., 2019). In contrast, expression of *TMO5*, *TMO5-LIKE 1* (*T5L1*), *TMO6*, *IQ-DOMAIN 15* (*IQD15*), *SOSEKI 1* (*SOK1*) and *WRKY17*, was shown to depend on MP activity (Schlereth et al., 2010; Möller et al., 2017; Yoshida et al., 2019).

Lineage tracing has suggested that the first vascular cells are specified in the early globular stage embryo (Scheres et al., 1994), when the embryo first contains three distinct cell layers in the lower tier (Fig. 1A). Indeed, we found almost all vascular reporters to be expressed in the lower inner cells at this stage, except for *TMO6* and *T5L1* (Fig. 1B). However, at this stage, most reporters were expressed in both the central cell layer and the surrounding ground tissue cells: *ATHB8*, *DOF6*, *PEAR1*, *WOL* and *ZLL* were expressed at apparently equal levels in both tissue types. In contrast, *IQD15* and *SOK1* showed lower levels of expression in the ground tissue (Fig. 1B). The only markers that were restricted to the innermost cell layer were *TMO5* and *SHR*, the expression of which could not be detected in the ground tissue (Fig. 1B). The broad expression of these vascular marker genes was only transient: within several cell division rounds, all vascular markers were restricted to the innermost cells, a pattern that was maintained in the postembryonic root (Fig. 1B). This suggests that, rather than being immediately restricted to a small number of innermost cells, the gene expression program associated with vascular identity is initially broad but becomes limited to inner cells over time. Although all 12 marker genes eventually become restricted to the vascular cells, it appears that not all are exclusively expressed in the vascular cells and there are multiple trajectories to their vascular-specific expression pattern.

The route to a vascular-specific expression pattern starts in the 16-cell stage embryo rather than at the early globular stage as previous reports have suggested. In previous work, inner lower tier cells at the 16-cell stage were shown to resemble their vascular daughter cells at the globular stage in terms of gene ontology term enrichment in transcriptomes (Palovaara et al., 2017). Indeed, we found that many vascular-specific marker genes start expression at the 16-cell stage, in which some showed expression in all cells (*ATHB* and *ZLL*) but most were exclusively expressed in the inner cells: *DOF6*, *IQD15*, *PEAR1*, *SOK1* and *WOL* (Fig. 1B; Fig. S1). Thus, as the eight-cell embryo divides to generate outer and inner cell layers at the 16-cell stage, inner cells activate vascular markers. Their ground tissue daughters initially retain the expression of some vascular markers and switch these off later.

Many of the vascular marker genes were originally identified as targets of auxin signaling, often regulated by MP (Schlereth et al., 2010; Möller et al., 2017). As a result, there is a bias towards auxin-regulated genes among the well-studied vascular marker genes. We therefore searched for novel marker genes in an unbiased manner. Vascular-enriched genes were selected based on their expression in

Development (2020) 147, dev186130. doi:10.1242/dev.186130

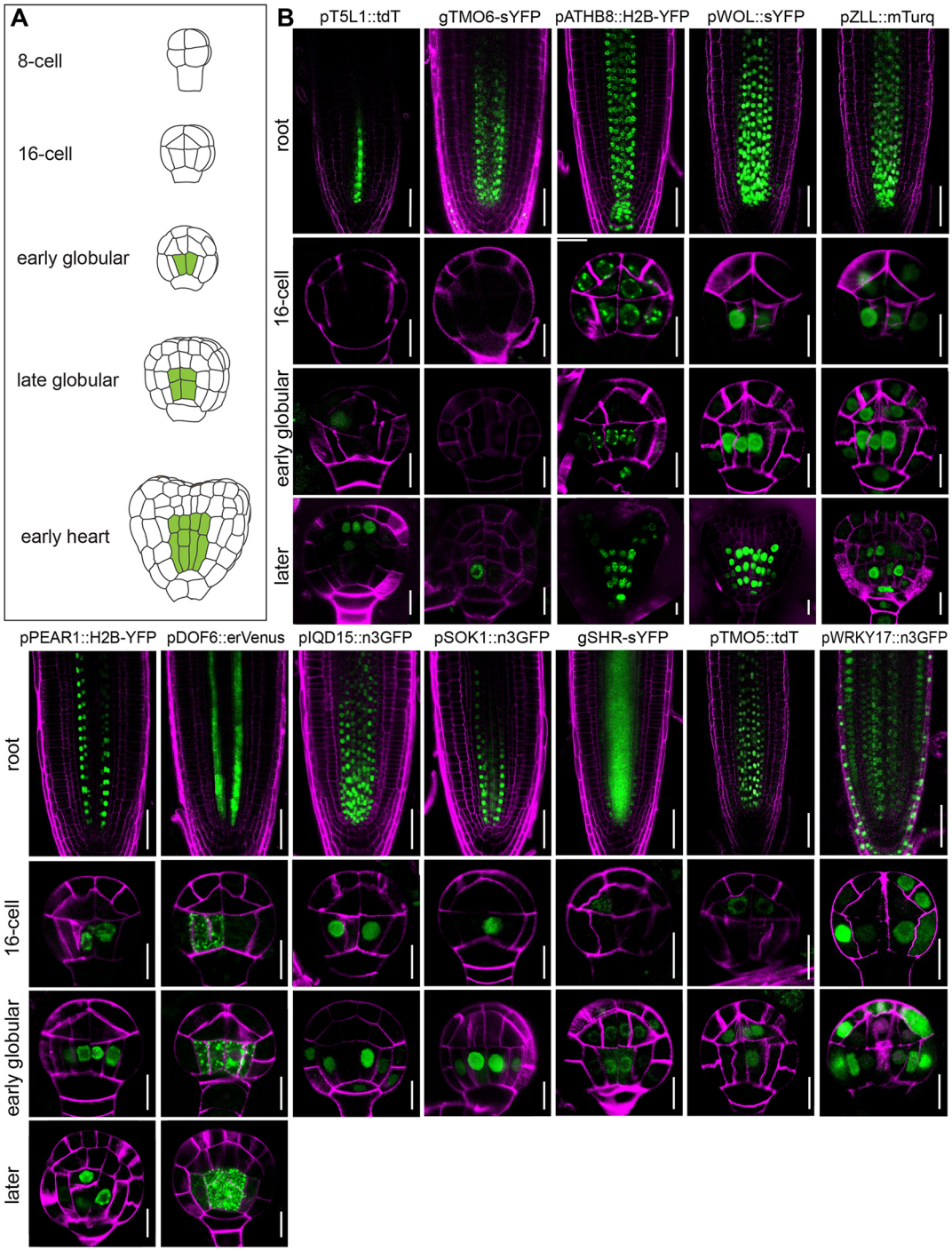

Fig. 1. Expression patterns of previously described vascular reporters. (A) Overview of stages of early embryogenesis. Cells previously discussed as vascular are marked in green. (B) Expression patterns of previously published vascular reporters in root and three stages of the early embryo. Images for WOL and ZLL are from the same root/embryo from a reporter line that carries both pWOL-sYFP and pZLL-mTurq. All reporters are transcriptional reporters except those for SHR and TMO6, which are translational fusions. Fluorescent protein signals are displayed in green, and cell wall staining in magenta. Roots are stained with PI and embryos with Renaissance 2200. Scale bars: 50 µm (root); 10 µm (embryo).

the early vascular cells, using a cell type-specific embryo transcriptome atlas (Palovaara et al., 2017) and additional publicly available vascular-specific transcriptome datasets (Fig. 2A) (Brady et al., 2007; Belmonte et al., 2013; Kondo et al., 2015; Melnyk et al., 2018). Transcriptional reporter lines were constructed to test the expression pattern of 36 potential marker genes and eventually five qualified as markers of vascular identity during embryogenesis (Fig. 2B). Expression of the remaining 31 genes could either not be detected during embryogenesis or was not limited to vascular cells in the embryo, while being specific to vascular tissue in the root (Fig. S2). Of the five selected reporters, *GATA20* and *AP2B3* expression started at the 16-cell stage, and at the early globular stage both were enriched in vascular cells (Fig. 2B). *AP2B3* expression peaked in vascular cells but could also be detected in surrounding cell layers (Fig. 2B), whereas *GATA20* expression showed vascular specificity (Fig. 2B). In the root tip, *GATA20* has been shown to be

Development (2020) 147, dev186130. doi:10.1242/dev.186130

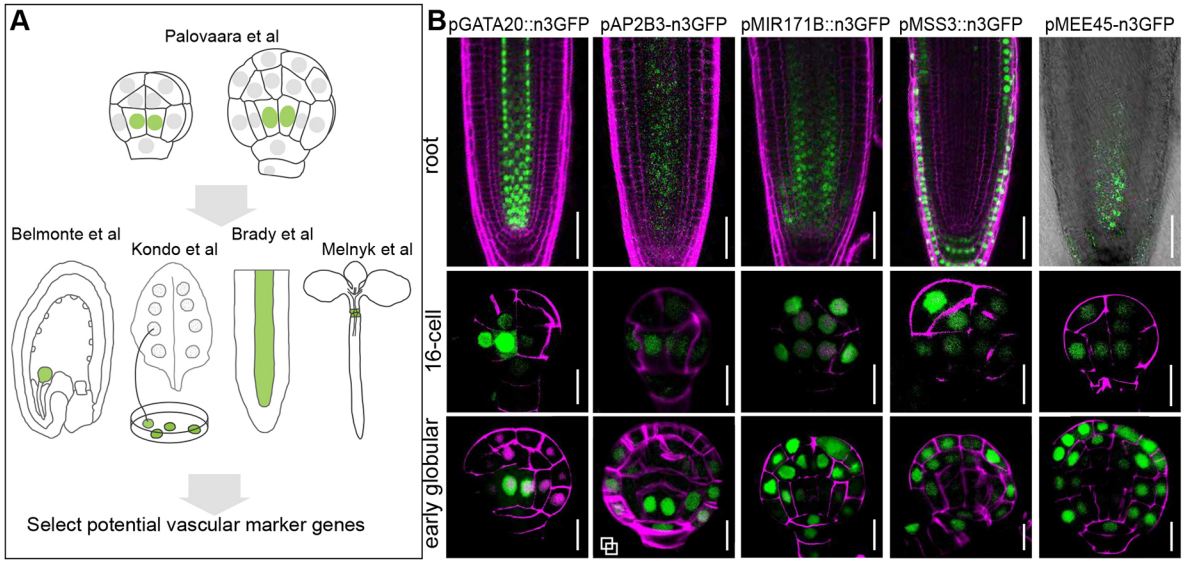

Fig. 2. Identification of novel vascular reporters. (A) Overview of transcriptomics datasets used for the selection of new vascular reporters. The studied tissue/cell type in each experiment is marked in green. (B) Expression patterns of new vascular reporters for the embryo. Fluorescent protein signals are displayed in green, and cell wall staining in magenta. Roots are stained with PI, embryos with Renaissance 2200. Overlapping square symbols indicate images resulting from a stack. Scale bars: 50 µm (root); 10 µm (embryo).

expressed in the phloem (Lee et al., 2006) and we found that this expression was broader in the vascular cells close to the quiescent center (Fig. S1B). The other three selected reporters, *MEE45*, *MIR171B* and *MSS3*, were expressed at the dermatogen stage in all cells, but at lower levels in the vascular cells within the embryo, thus marking vascular cells with their expression minimum. *MIR171B* and *MSS3*, like *WRKY17*, were first expressed at the eight-cell stage and thus appeared to be repressed in the first vascular cells (Fig. S1). Because these genes have an inverted expression pattern compared with the expectation for a vascular gene, we will refer to these genes as 'inverse' markers of vascular identity in the embryo, indicating that their expression minimum, rather than their maximum, marks the vascular cells. This pattern is similar to that of *WRKY17*, a target of MP (Möller et al., 2017) (Fig. 1B). However, although *WRKY17* was expressed broadly in the root meristem, *MEE45*, *MIR171B* and *MSS3* showed tissue-specific expression in the root (Fig. 2B). Beyond resolving the ontogeny of vascular tissue identity in the embryo, our detailed analysis of vascular-specific markers also shows that there are significant differences in gene expression restriction to the vascular tissue between embryo and root. Hence, initial specification and maintenance of tissue identity seem to be associated with different gene expression patterns.

Auxin signaling through MP is necessary, but not sufficient, for initiation of vascular identity

Auxin signaling plays many key roles in plant development and one of the clearest is its contribution to vascular development. We sought to investigate the role of auxin signaling in the specification of vascular identity in the early embryo. To this end, we expressed a nondegradable version of the BDL (BODENLOS/IAA12) protein to block MP activity (Hamann et al., 2002; Weijers et al., 2006), while examining markers of vascular identity (Fig. 3A-B). As *bdl* expression in the entire embryo results in early developmental defects (Rademacher et al., 2012; Yoshida et al., 2014), we employed two-component gene activation and selectively expressed *bdl* in vascular cells using the Q0990-GAL4; UAS-erGFP driver line (Fig. 3A) (Haseloff, 1999). The GAL4 driver in the Q0990 line is inserted near the ZLL gene (Radoeva et al., 2016) and erGFP thus reports *ZLL* expression. Vascular markers were introduced into the Q0990 background and crossed with a line containing GAL4-dependent UAS-*bdl* (Weijers et al., 2006). The domain of *bdl* expression was marked by ER-localized GFP, whereas the vascular markers were reported by nuclear GFP fluorescence (Fig. 3A,B).

Embryos in which *bdl* was expressed in the vascular cells often showed altered ground tissue division orientation, as previously reported (Möller et al., 2017) (Fig. 3B), indicating that auxin signaling was successfully inhibited. However, erGFP expression was not affected in *bdl*-expressing embryos (Fig. 3B), indicating that maintenance of *ZLL* expression in presumptive vascular cells does not depend on the auxin response. Crosses of the Q0990-GAL4 line with Col-0 wild type resulted in no such changes in division orientation. *bdl* expression led to 96% (n=24) of the observed embryos lacking nuclear *SOK1* expression, whereas almost all wild-type crossed embryos showed normal *SOK1* expression. As *SOK1* is regulated by MP (Möller et al., 2017; Yoshida et al., 2019), this further confirms the repression of MP activity. However, not all vascular characteristics were absent from the inner cells. In Q0990≫*bdl* embryos, *GATA20* expression was absent in about half (54%, n=13) of the embryos, but remained present in the other half, indicating that, in many embryos, repression of vascular identity was incomplete, as was supported by normal *ZLL* expression. In addition, expression of the inverse marker *MIR171B* was mostly unchanged in Q0990≫*bdl* embryos (Fig. 3B). These findings indicate that, when auxin signaling is blocked in inner cells, vascular identity is compromised but not abolished. The remaining vascular program is insufficient for further proliferation and development (Berleth and Jürgens, 1993; Hamann et al., 1999; Weijers et al., 2006; De Rybel et al., 2013; Möller et al., 2017), thus we conclude that auxin signaling through MP is essential for functional vascular tissue specification.

After confirming that auxin signaling is required for specification of vascular identity, we next asked whether it is also sufficient. Although differences in auxin activity across cell layers in the early embryo, as measured by the R2D2 and *DR5v2* reporters (Liao et al., 2015), are small, there is a clearly defined gradient with high levels in central and lower levels in peripheral cells (Möller et al., 2017)

Development (2020) 147, dev186130. doi:10.1242/dev.186130

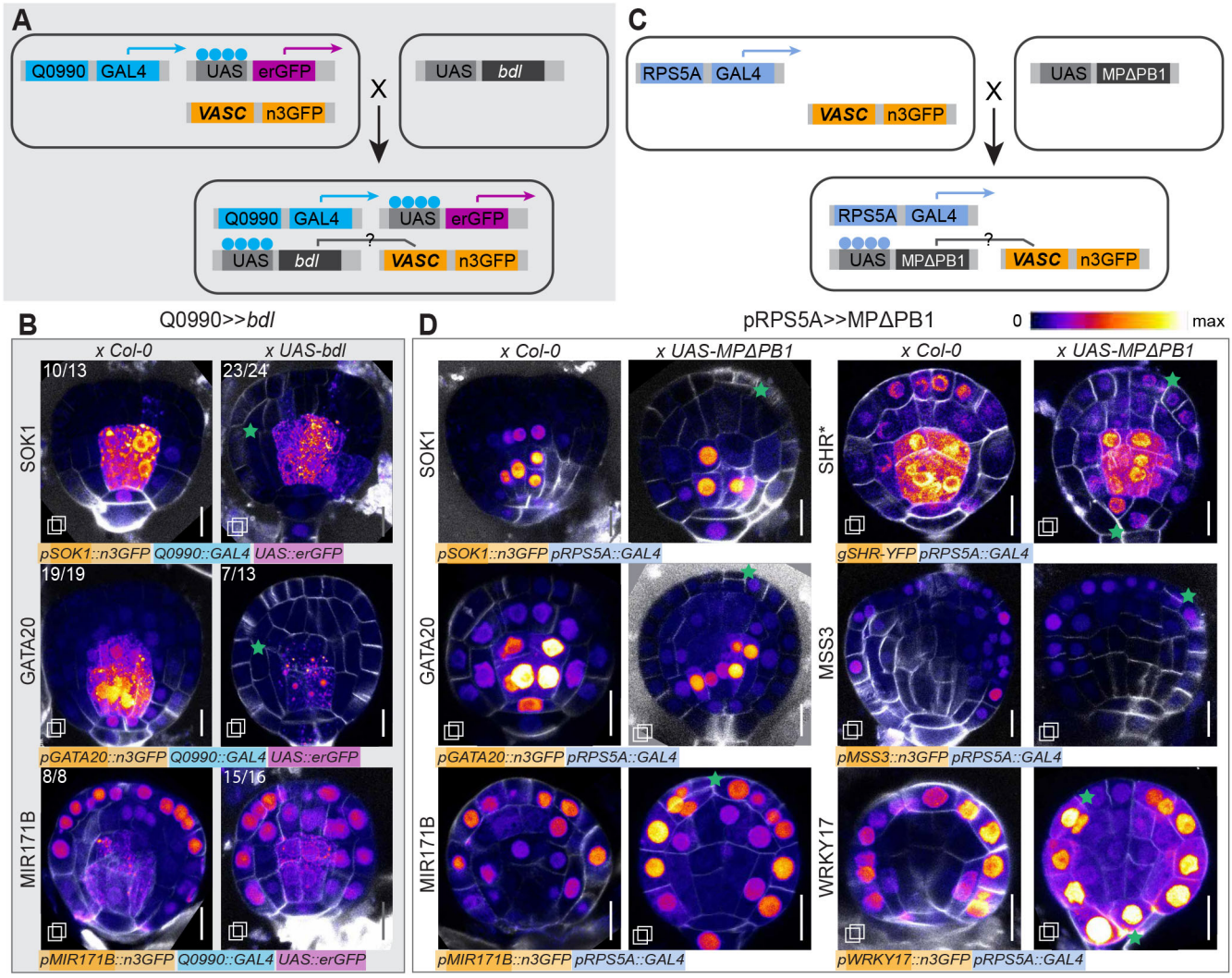

Fig. 3. The role of the auxin response in embryonic vascular gene expression. (A) Diagram showing the experimental setup for Q0990≫*bdl* crosses. (B) Embryos resulting from crosses between a line containing Q0990::GAL4, UAS::erGFP and a vascular reporter, and either Col-0 or a line containing UAS::*bdl*. Numbers in the top left corner of each panel indicate the fraction of embryos observed with the pattern displayed. Green stars indicate altered ground tissue division orientation. (C) Diagram showing the experimental setup for pRPS5A≫UAS::MPΔPB1 crosses. (D) Embryos resulting from crosses between a line containing pRPS5A::GAL4 and a vascular reporter, and either Col-0 or a line containing UAS::MPΔPB1. Fluorescent protein signals are visualized using the Fire lookup table (see color key bar). Green stars indicate altered division planes in epidermal cells and in the hypophysis. Embryos are stained with Renaissance 2200 (white). Overlapping square symbols indicate images resulting from a stack. In A, vascular reporters are represented by nuclear signal, whereas the expression domain of the Q0990 reporter (UAS-erGFP) is marked by ER-localized GFP. Scale bars: 10 µm.

(Fig. S3). We asked if this small difference in auxin signaling between central and peripheral cells in the embryo is sufficient to restrict (vascular) identity to inner cells. We therefore expressed a version of MP that cannot be inhibited by auxin-dependent Aux/IAA proteins and that is hyperactive (MPΔPB1) (Krogan et al., 2012) from the ubiquitous *RPS5A* (*RIBOSOMAL PROTEIN 5A*) promoter (Weijers et al., 2001) using the GAL4-UAS system (Fig. 3C). Embryos with ubiquitous MPΔPB1 expression often showed altered division planes in epidermal cells and occasionally in the hypophysis (Fig. 3D), indicating the effectiveness of transgene expression. However, ectopic MPΔPB1 expression did not induce ectopic vascular marker expression. Expression of vascular genes (*GATA20*, *SHR* and *SOK1*) remained restricted to the vascular cells; likewise, inverse markers of identity (*MIR171B*, *MSS3* and *WRKY17*) still showed an expression minimum in the vascular cells (Fig. 3D). These results show that the ectopic auxin response can induce changes in cell division orientation, but is insufficient for inducing vascular tissue specification in the early embryo. This suggests that unknown additional factors limit the domain of vascular identity.

Identification of transcriptional regulators of vascular gene expression

Given the co-expression of vascular marker genes in the embryo and in the post-embryonic vasculature, it is likely that there are common regulators. To identify transcription factors that bind multiple vascular gene promoters, we performed an eY1H assay (Gaudinier et al., 2011; Reece-Hoyes et al., 2011). Promoters from 14 of the aforementioned vascular reporter genes were screened against a customized collection of 2037 transcription factors and other DNA-binding proteins in an all-by-all setup (Table S1). Among the 32,592 interactions tested, 1111 were positive. Combining all interactions resulted in a network comprising 14 promoters and 382 transcription factors (Fig. S4; supplementary Dataset S1; Table 1).

Development (2020) 147, dev186130. doi:10.1242/dev.186130

Table 1. Number of interactions recorded per promoter screened

Locus	Promoter	Number of interactors
AT1G05577	*SOK1*	69
AT1G11735	*MIR171B*	94
AT1G68810	*T5L1*	125
AT2G01830	*WOL*	11
AT2G18380	*GATA20*	82
AT2G24570	*WRKY17*	79
AT2G43290	*MSS3*	74
AT3G15210	*ERF4*	90
AT3G25710	*TMO5*	110
AT3G49380	*IQD15*	8
AT4G32880	*ATHB8*	78
AT4G37650	*SHR*	94
AT5G43810	*ZLL*	123
AT5G60200	*TMO6*	77

This network contained a large number of transcription factors that could bind to many of the vascular promoters. For in-depth analysis, we therefore selected the six vascular promoters that each had more than 25 interactors and showed the most prominent vascular specificity in the early embryo (Fig. 4A). These six consisted of: three vascular-specific marker genes (*GATA20*, *SOK1* and *ZLL*); and three vascular inverse marker genes (*MIR171B*, *MSS3* and *WRKY17*). The network that contains these promoters and their interactors comprises 221 transcription factors and 521 interactions (Fig. 4A). If there is a common vascular transcriptional program, it is likely that multiple vascular genes are regulated by a common set of transcription factors. We therefore parsed the interaction network to identify such common transcription factors as potential regulators of vascular identity specification.

A large number of transcription factors were identified to interact with the majority of these promoter sequences. The majority of these transcription factors bind to both sets of promoters (vascular specific and inverse), whereas only a few can bind to only one set. CUC2 (CUP-SHAPED COTYLEDON 2; Aida et al., 1997) and IDD12 INDETERMINATE-DOMAIN 12) can bind to three or more vascular-specific markers but no inverse markers. JAG (JAGGED; Ohno et al., 2004), DRN (DORNROSCHEN; Kirch et al., 2003) and ARR1 (RESPONSE REGULATOR 1; Sakai et al., 2001) bind to two or more vascular inverse markers but no vascular-specific markers (Fig. 4A). However, these transcription factors are a small minority: in general, the vascular-specific and -inverse promoters have highly similar sets of transcription factors binding to their promoters, despite having very different expression patterns. When we performed clustering on the promoters based on their interactor set, we found that vascular-specific and vascular-inverse markers did not have distinct sets of interactors (Fig. 4C). These findings suggest a large set of transcription factors that could act in a complex gene regulatory network (GRN) controlling vascular identity specification. It should be noted though that both sets of promoters show differential expression between vascular and nonvascular cells, and it is possible that the same transcription factors (or related proteins) could act as vascular-specific activators or repressors.

To identify candidate regulators of vascular identity specification, we selected 20 transcription factors from the network. This selection was performed in two steps. First, transcription factors were discarded that: (1) bound to few vascular promoters; (2) were expected to be false positives based on their promiscuous binding profiles in previous screens (Gaudinier et al., 2018; Taylor-Teeples et al., 2015); or (3) were most likely not expressed during embryogenesis based on transcriptomics data (Belmonte et al., 2013; Schlereth et al., 2010). This approach resulted in a list of 50 transcription factors. Next, each transcription factor was scored for: (1) expression during vascular development and early embryogenesis; (2) the number of vascular promoters bound; (3) diversity of expression patterns bound; and (4) vascular promoter binding in published DNA affinity purification sequencing (DAP-seq) data (O'Malley et al., 2016). For further analysis, we selected the top 20 transcription factors ranked by cumulative score (Table S3; Fig. 4B).

A candidate regulator of identity would be expected to be present at the time and place that specification takes place. To ascertain the presence of candidate regulators during embryogenesis, translational fusions of genomic fragments to YFP were created and observed for 17 of these 20 transcription factors. These revealed that ten candidate regulators were indeed present at the 16-cell stage in the pro-embryo (Fig. 5A). The remaining seven were either not detected during embryogenesis or not at the correct time or location (Fig. S5). The majority of the ten candidate regulators expressed in 16-cell embryos are present uniformly in the nucleus, except for members of the GeBP (GL1 ENHANCER BINDING PROTEIN) family, which accumulate in foci within the nucleus, similar to previous reports (Fig. 5A) (Curaba et al., 2003). No conspicuous differences between cell types could be found in the early embryo, in either protein quantity or localization. This indicates that, if these candidates contribute to specifying vascular identity, their cell-specific action is not the result of protein level or location. Instead. an unknown mechanism might contribute to cell-specific activity.

GBF1 and GBF2 can interact with MP

To determine whether any of the candidate regulators could induce or repress gene activity during vascular tissue specification, each was expressed in meristematic cells with the *RPS5A* promoter (Weijers et al., 2001), either as native cDNA or as a fusion with a dominant SRDX repressor motif. Misexpression of several resulted in either lethal or mild developmental phenotypes, but none of the identified candidate regulators suppressed or ectopically induced vascular tissue differentiation (Fig. S6). Therefore, it is unlikely that any of these candidates act in isolation to control vascular tissue initiation. A more likely explanation is that identity is controlled by a complex GRN, in which the unique interactions between individual regulators provide cell-type specificity.

In our efforts to understand the mechanisms of gene regulation by MP, we immunoprecipitated MP-containing protein complexes from root tips in an MP-GFP transgenic line whose functionality had been validated (Schlereth et al., 2010). In this experiment, we identified GBF2 (G-BOX BINDING FACTOR 2) as a potential interactor of MP-GFP (Table S2). As both MP and GBF2 are candidate regulators of vascular identity specification, we decided to follow up on this interaction. Immunoprecipitation of GBF2-YFP and its homolog GBF1-YFP, followed by mass spectrometry, did not recover MP, presumably due to the very low abundance of MP, but did confirm previous observations that G-class bZIP proteins can heterodimerize extensively (Fig. S7). To test MP-GBF interactions more directly, we performed split-YFP assays [bimolecular fluorescence complementation (BiFC)] (Hu et al., 2002; Walter et al., 2004) in *Nicotiana benthamiana*. Both GBF2 and GBF1 could interact with MP (Fig. 5B,C; Fig. S8). Interestingly, this interaction was not restricted to MP: ARFs of all three major classes [A, B and C: Okushima et al. (2005); Finet et al. (2013)] could interact with both GBF2 and GBF1 (Fig. 5B;

Development (2020) 147, dev186130. doi:10.1242/dev.186130

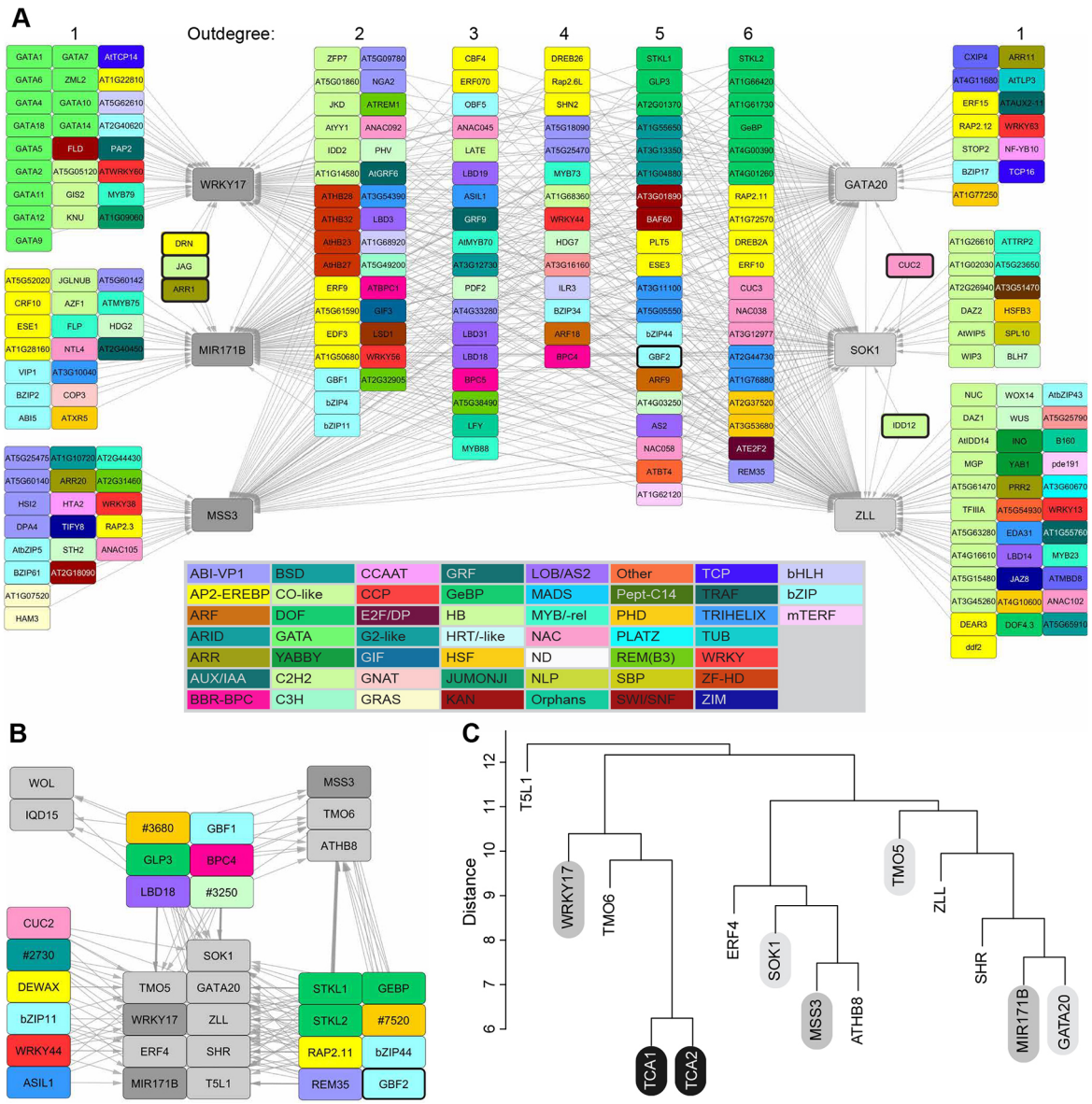

Fig. 4. Partial yeast one network and selection, and candidate regulators of vascular identity. (A) A yeast one-hybrid network showing all interactors of six out of 14 vascular promoters screened. Nodes representing transcription factors are colored according to their transcription factor family (see inset), and are grouped by outdegree. Nodes representing promoters are colored light (vascular specific) or dark (vascular inverse) gray. (B) Network overview of the 20 candidate regulators of vascular identity with all 16 vascular promoters screened. Colors are as in A. (C) Dendrogram resulting from hierarchical clustering of promoters by interactor set. Branch length indicates distance/similarity in the interactor set. Two promoters from an unrelated screen (TCA1 and TCA2) were included as an outgroup.

Fig. S8), and the interaction domain was mapped to the ARF DNA-binding domain (Fig. 5B,C; Fig. S8).

GBF proteins have been reported to be involved in the responses to blue light and in leaf senescence (Singh et al., 2012; Smykowski et al., 2010; Mallappa et al., 2006; Giri et al., 2017). However, *gbf1*, *gbf2* and *gbf3* single and double mutants show no developmental phenotypes (Fig. S9). This is likely a result of genetic redundancy: the bZIP G-class contains five members and double mutants show increased expression of close homologs (Jakoby et al., 2002; Dröge-Laser et al., 2018) (Fig. S9). A triple mutant could not be recovered from plants that were homozygous for *gbf1* and *gbf3* or from plants that segregated *gbf2*, suggesting that a lack of all three proteins may result in lethality. Indeed, disruption of a GRN underlying vascular identity specification would likely result in early developmental arrest. Overexpression using *RPS5A* or *35S* promoters caused pleiotropic developmental defects. pRPS5A≫GBF2-SRDX plants were often sterile, whereas 35S::GBF1/2 plants had round leaves and showed delayed flowering (Figs S5 and S9). However, no ectopic vascular tissue differentiation was observed. These findings indicate that GBF1/2 protein quantity alone does not specifically limit vascular tissue specification.

GBFs bind to Gboxes close to auxin response elements to modulate auxin responsive expression

GBF2 and GBF1 physically interact with the DNA-binding domain (DBD) of ARFs, and thus have the potential to co-regulate auxin-responsive genes. Interactions among transcription factors can lead to cooperative DNA binding if both transcription factors can bind to cognate DNA elements in close proximity. Indeed, Gbox motifs

Development (2020) 147, dev186130. doi:10.1242/dev.186130

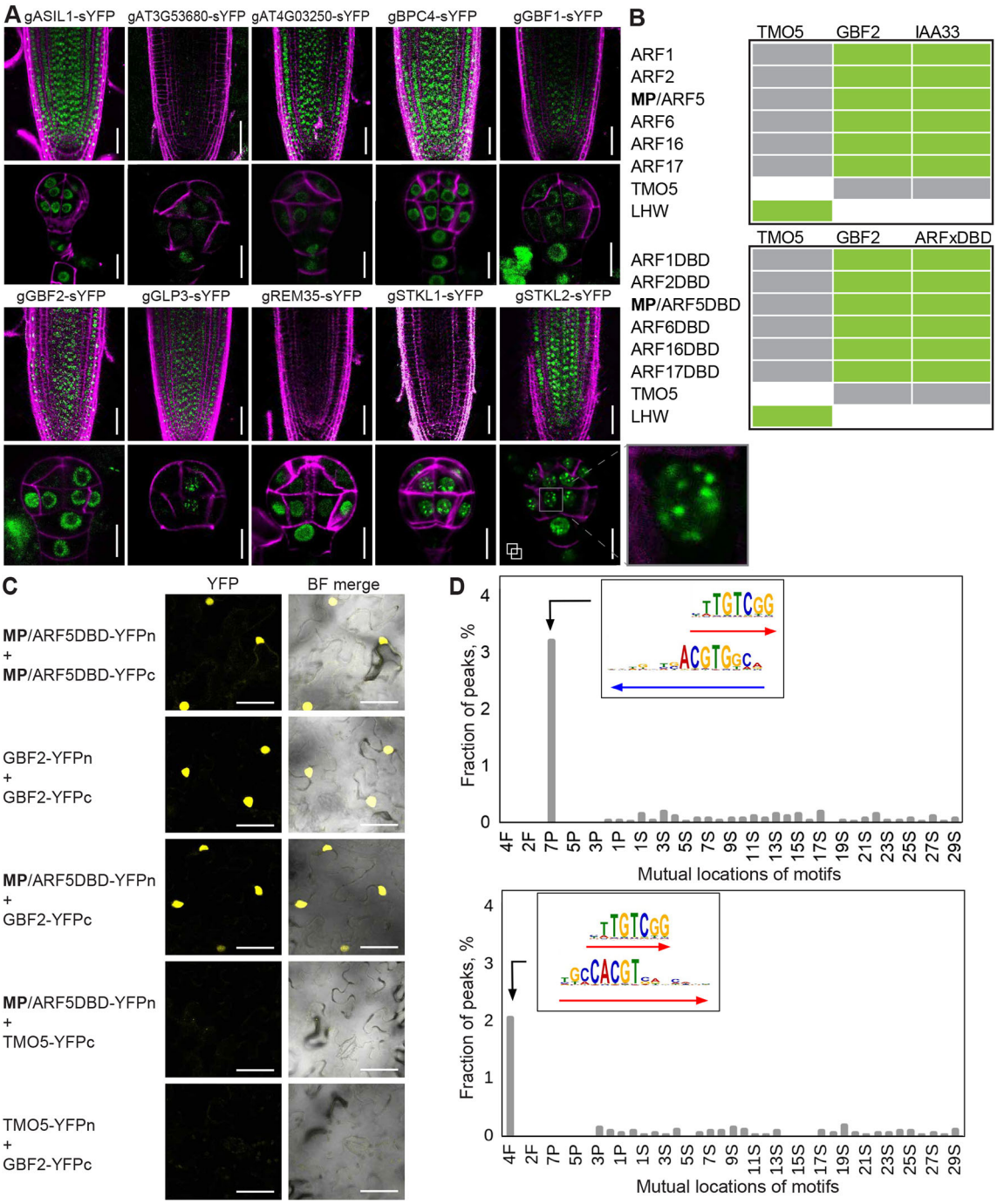

Fig. 5. Protein localization and interactions of candidate regulators of vascular identity. (A) Translational reporter lines of ten candidate regulators in the root tip and early pro-embryo. Gray square indicates the inset highlighting STKL2 expression in foci within the nucleus. Fluorescent protein signals are displayed in green, and cell wall staining in magenta. Roots are stained with PI, and embryos with Renaissance 2200. (B) Overview of split-YFP (BiFC) results indicating that GBF2 can interact with the full-length protein and DBD of six different ARFs. Green indicates that interaction was observed, whereas gray indicates no interaction. (C) Selected images of split-YFP (BiFC) assays showing the interaction between the DBD of MP/ARF5 and GBF2. (D) Distribution of potential MP/bZIP68 composite elements within MP-binding regions taken from DAP-seq. *x* axis numbers reflect the number of nucleotides, F, full overlap; P, partial overlap; S, spacer. Top: MP/bZip68 everted composite element distribution. Bottom: MP/bZIP68 direct composite element distribution. Scale bars: 50 µm (root) or 10 µm (embryo) (A); 75 µm (tobacco leaf) (C).

were found to be enriched in close proximity to auxin response elements (AuxREs) (Weiste and Dröge-Laser, 2014; Ulmasov et al., 1995) and they are overrepresented in auxin-responsive and ARF-binding regions (Berendzen et al., 2012; Cherenkov et al., 2018). To test the co-occurrence of ARFs and G-class bZIPs motifs, we applied the Motifs Co-Occurrence Tool (MCOT) (Levitsky et al., 2019) to ARF5 and ARF2 peaks taken from genome-wide DAP-seq profiles (O'Malley et al., 2016). We analyzed all possible combinations of AuxREs (ARF2/5 motifs) and Gboxes (GBF3 and bZIP16/68 motifs) with any overlap or spacer lengths below 30 nucleotides, and found that bZIP68 and ARF5 motifs overlap (*P*-value<5E-40) (Fig. 5D).

Development (2020) 147, dev186130. doi:10.1242/dev.186130

To investigate the function of these linked motifs, we selected three vascular promoters that contained clear AuxRE and Gbox motifs in close proximity: with an overlap (WRKY17), a short spacer (TMO5) and a long spacer (GATA20) (Fig. 6A). Transcriptional reporters with mutated promoters were generated to determine the contribution of the AuxRE-Gbox motif to vascular gene expression domain and level. Removing the complete AuxRE-Gbox motif from the promoters of *GATA20*, *TMO5* and *WRKY17* resulted in a strong and significant reduction of fluorescence in transgenic roots (Fig. 6C-E). For the *WRKY17* reporter, this reduction was more significant in the vascular bundle compared with the rest of the root meristem, resulting in a changed vascular/nonvascular signal ratio (Fig. 6E-H). This suggests that, for this promoter, the overlapping AuxRE-Gbox motif controls expression levels specifically in vascular cells. Removing only the Gbox had a smaller effect (Fig. 6C-E). Mutated *GATA20* and *TMO5* promoters in which the adjoining Gbox had been removed did not show a significant decrease in fluorescence, but instead resulted in increased variation in expression level among transgenic lines (Fig. 6C,D). Thus, the Gboxes in these

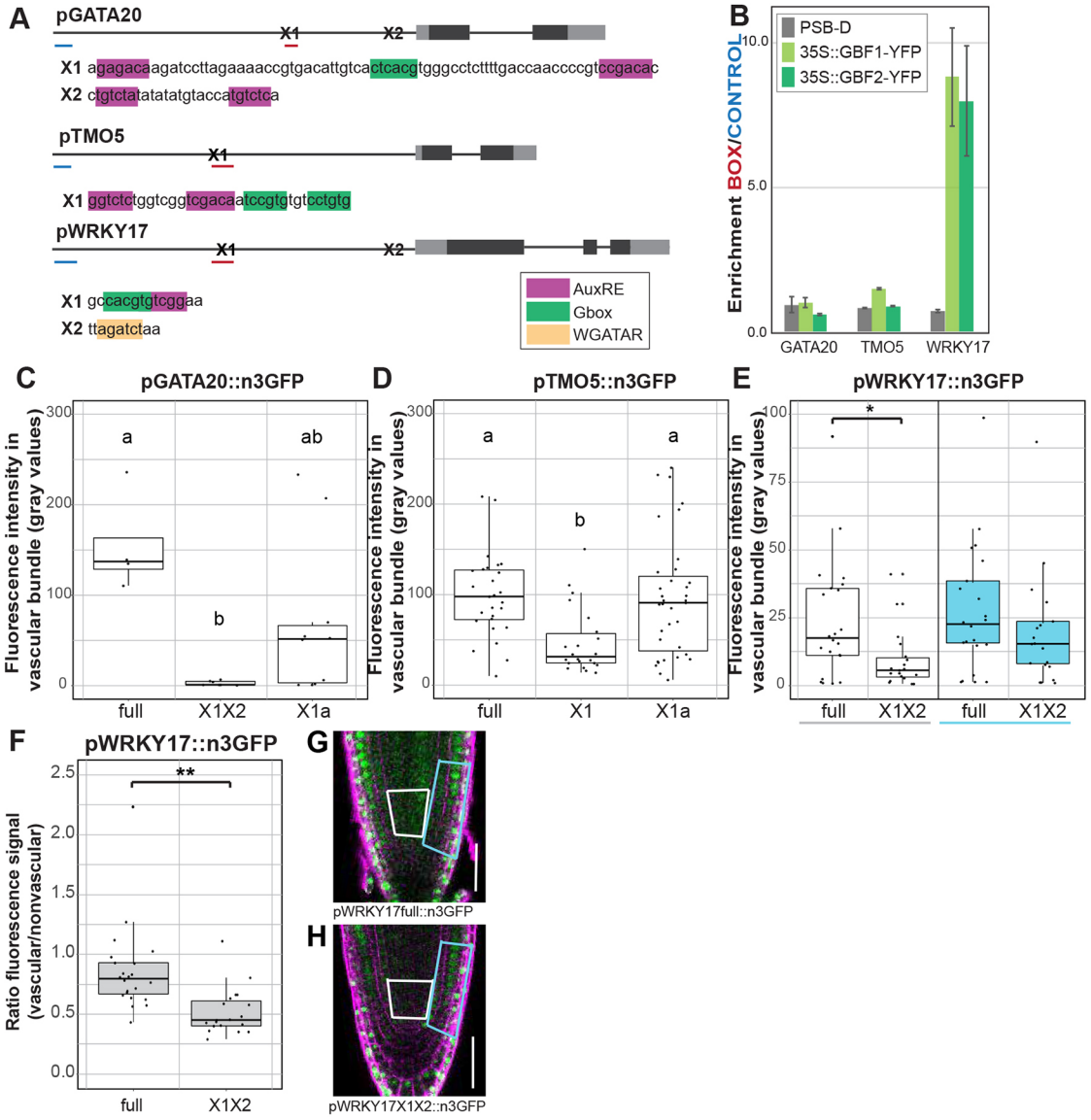

Fig. 6. Gboxes can be bound by GBF2 and are needed for stable vascular expression. (A) Schematic overview of the promoter sequences of *GATA20*, *TMO5* and *WRKY17*. X1 and X2 indicate regions containing TF-binding sites. Blue and red lines indicate control regions and Gbox regions used for ChIP-qPCR, respectively. (B) ChIP-qPCR performed on *Arabidopsis* cell cultures expressing either GBF1-YFP or GBF2-YFP. Relative enrichment of the BOX regions compared with CONTROL regions. Data are mean±s.e.m. (C-E) Boxplots displaying fluorescence intensity of transcriptional reporter lines. Each plot compares the mean fluorescence in the measured cells for T1 roots containing full-length or truncated promoters of GATA20 (C), TMO5 (D) and WKRY17 (E). Each point is the mean fluorescence in the early vascular cells measured from one independent T1 root. For the WRKY17 promoter, two areas were measured: the vascular bundle (white) and adjacent nonvascular cells (blue). For box plots, the box marks the first and third quartiles, split by the median; whiskers extend to a maximum of 1.5× the interquartile range beyond the box. **P*<0.05, ***P*<0.001; two-sided, unpaired Student's *t*-test. One-way analysis of variance (ANOVA) followed by Tukey's honest significant difference (HSD) test was performed to compare differences in fluorescence intensity. Samples were classified into up to three categories per experiment (a/ab/b). Results from the Tukey's HSD test are listed in Table S4. (F) The ratio of WRKY17-driven GFP signal in the vascular cells compared with signal in the nonvascular cells. (G,H) Expression patterns in representative WRKY17 T1 roots. Boxes indicate the regions in which fluorescent signal was measured. Scale bars: 50 µm.

Development (2020) 147, dev186130. doi:10.1242/dev.186130

promoters appear to be contributing to the expression stability instead of to absolute vascular expression levels. As members of several transcription factor families can bind to Gboxes (Schindler et al., 1992; Lian et al., 2017; O'Malley et al., 2016), it is unclear whether GBF2 is the factor contributing to stability of vascular gene expression.

Next, we tested whether GBF2 alone could bind to the Gboxes present in vascular promoters. ChIP-qPCR on suspension cell cultures overexpressing GBF2-YFP confirmed that GBF2 could bind to the Gbox motif in the *WRKY17* promoter, but could not confirm the same for the *GATA20* and *TMO5* promoters (Fig. 6B). Instead, it is possible that GBF2 and MP both need to be present to interact with the promoters of these two genes.

If GBF2 can bind to vascular promoters and co-regulate vascular gene expression, its overexpression should affect the regulation of vascular genes. To test this directly, we generated protoplasts from vascular reporter lines p*VASC::*n3GFP (VASC being either GATA20, TMO5 or WRKY17), and transfected these with a combination of 35S::GBF2-mTurquoise2, 35S::MPΔPB1-mScarlet-I and corresponding empty vectors to determine their effects on target promoter activity (Fig. 7D-F). MPΔPB1 was used to overcome any auxin-dependent inhibition. Overexpression of only GBF2-mTurquoise2 had no effect on the promoter activity of *GATA20*, *TMO5* and *WRKY17*. In contrast, expression of MPΔPB1-mScarlet-I resulted in increased *TMO5* promoter activity and decreased *WRKY17* promoter activity (Fig. 7B,C). This effect disappeared when GBF2 was co-expressed with MPΔPB1, suggesting that GBF2 acts by restricting MP activity, probably via competitive binding with the overlapping AuxRE-Gbox motif. This was not the case for the GATA20 promoter, the activity of which was decreased by both MPΔPB1-mScarlet-I and by MPΔPB1-mScarlet-I combined with GBF2-mTurquoise2 (Fig. 7A). These findings suggest that the interaction between GBF2 and MP depends on promoter context, yet reflects a functional interaction that contributes to the regulation of vascular genes.

DISCUSSION

Vascular tissues play a central role in plant development. Anatomical, physiological and genetic studies contribute to our understanding of vascular tissue development and key aspects of its regulation. Although significant insights have been gained into the regulation of cell identity specification, pattern formation, growth and differentiation within the vascular tissue, a key unresolved issue is how this tissue is initially specified from nonvascular precursor cells. From lineage tracing in *Arabidopsis*, it is clear that the vascular lineage has its origins in the early embryo (Scheres et al., 1995); however, the origin of embryonic vascular tissue has thus far not been characterized molecularly. Here, we have used a panel of vascular marker genes to map the ontogeny of vascular tissue identity from the embryo to postembryonic tissues. First, we traced its initiation to the 16-cell stage embryo. At this stage, the outer cells acquire protoderm identity (Abe et al., 2003), and we found that the inner cells express multiple vascular marker genes, identifying these cells as the first with vascular attributes. None of the ground tissue markers we have analyzed was present in the inner lower tier cells of

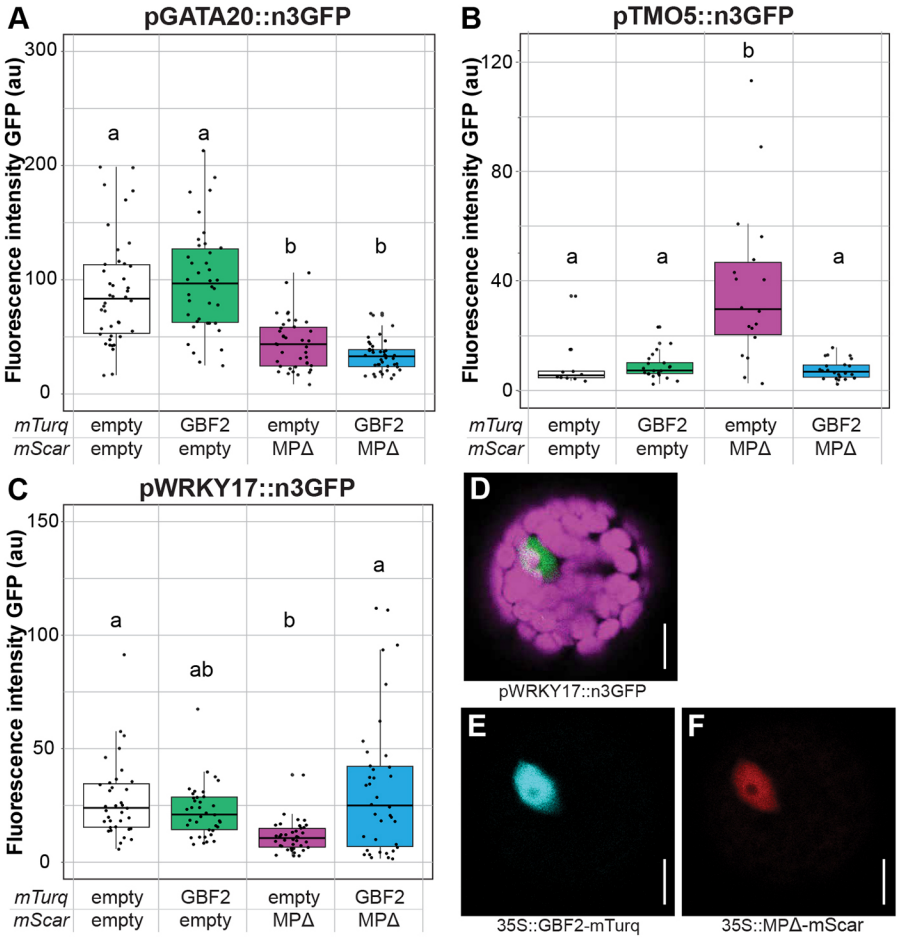

Fig. 7. GBF2 modulates MPΔ induced vascular gene expression. (A-C) Boxplots displaying intensity of green fluorescence in nuclei of protoplasts transformed with two misexpression constructs that were either empty or contained GBF2 or MPΔPB1. Protoplasts were generated from leaves that expressed pGATA20::n3GFP (A), pTMO5::n3GFP (B) or pWRKY17::n3GFP (C). One-way analysis of variance followed by Tukey's honest significant difference (HSD) test was performed to compare changes in fluorescence intensity. Samples were classified into up to three categories per experiment (a/ab/b). Results from the Tukey's HSD test are listed in Table S4. Each assay was performed twice with similar results. (D-F) Fluorescence signals detected in protoplast assays. Pink, chloroplasts; green, GFP; cyan, mTurquoise2; red, mScarlet-I. Scale bars: 75 µm.

Development (2020) 147, dev186130. doi:10.1242/dev.186130

the 16-cell stage embryo. These findings are in line with results of a recent transcriptome study that found that the transcriptome of these (inner) cells is similar to that of the later vascular cells (Palovaara et al., 2017). This suggests that, instead of vascular and ground tissue identities emerging simultaneously, the first ground tissue cells are the daughters of the first vascular cells.

We found that the transcriptional dynamics and progression are vastly different among genes that later mark the vascular domain. Some genes, such as *DOF6*, *GATA20*, *SOK1* and *TMO5*, quite strictly mark the vascular cells, whereas others, such as *ATHB8* and *ZLL*, can be found in adjacent cell types during early embryogenesis. The strict vascular markers provide better tools for studying the emergence of vascular identity, at least in the context of embryogenesis. The dynamic expression patterns of vascular marker genes suggest that vascular tissue identity is not a uniform trait that exists across developmental stages, urging us to reconsider how we view the development of cell identity over time. Features that distinguish embryonic versus postembryonic vascular cells are the co-expression of xylem- and phloem-specific marker genes, and the lack of expression from vascular inverse markers. This suggests that initial vascular tissue identity in the embryo is a temporary state that does not persist. Indeed, in the postembryonic vascular cells, different vascular cell types are highly divergent, a trait that is emphasized by recent advances in single cell (sc)RNAseq. In scRNAseq experiments performed on roots, xylem and phloem cells form distinct clusters; however, vascular tissues as a whole do not form a cluster that is separated from the two other 'major' tissue identities: ground tissue and epidermis (Ryu et al., 2019; Shulse et al., 2019; Denyer et al., 2019). It is questionable whether cells in the postembryonic vascular bundle have, or need, a common identity. Instead, the brief existence of a 'general' primordial multipotent vascular identity may only be needed when new vascular bundles are initiated: to ensure proper placement of the vascular bundle as a whole and to establish the cambial cells. Future scRNAseq experiments on the embryo and, for example, on wounded stems or graft junctions (Melnyk et al., 2018) could help address this issue.

There is a strong connection between *de novo* vascular tissue formation and auxin activity. Lack of auxin signaling results in impaired vascular tissue development, whereas the application of exogenous auxin can induce the formation of new vascular bundles (Sachs, 1969; Krogan et al., 2012; Donner et al., 2009; Jacobs, 1952). Auxin and its key transcriptional effector MP are therefore often regarded as master regulators of vascular tissue development (Brackmann et al., 2018). Here, we asked whether this prominent role also pertains to the earliest steps in vascular tissue specification in the embryo. We found that auxin signaling in the central cells of the embryo is indeed required for the complete establishment of the vascular transcription program. This conclusion is supported by an earlier transcriptome analysis, in which many vascular genes were downregulated in embryos where the auxin response inhibitor *bdl* was expressed in the inner cells marked by the Q0990 driver (Möller et al., 2017; Radoeva et al., 2016). Interestingly though, several vascular marker genes, including the *ZLL* gene, persisted even upon auxin response inhibition. This suggests that for part of the vascular program, the auxin response is not required after the initial specification event. Conversely, we found that auxin signaling through MP is not sufficient to induce vascular tissue identity specification outside of the normal vascular domain. It should, however, be noted that a dominant-active version of MP lacking its C-terminal PB1 domains was used. It is possible that interactions with the PB1 domain, other than Aux/IAA inhibition – such as, for example, homo-oligomerization (Nanao et al., 2014) – are required for the activity of MP in vascular tissue development. Nonetheless, this result suggests that, in addition to the auxin response, there must be additional, yet undiscovered, factors that determine which cells acquire vascular tissue identity. Given the small size of the embryo, a system built on a set of regulators would also provide a more robust mechanism for the regulation of identity than a single master regulator of identity.

Using an eY1H assay, we identified ten transcription factors that can bind to a large number of vascular promoter sequences and are also present at the moment of vascular identity specification. Although the exact roles and relations of these transcription factors remain unclear, they could be part of the GRN controlling vascular tissue specification and provide a new entry point into studying its regulation. A complex GRN would provide a robust system for the initial specification of identity. Although it is clear that auxin signaling through MP is necessary, other candidate regulators of identity have not yet been untangled. As single perturbations of other components had little effect, we decided to explore the link between MP and a new candidate regulator: GBF2 and its close homolog GBF1.

GBF1 and GBF2 not only bind multiple vascular gene promoters but they also interact with the DBDs of ARF proteins of all three major classes [A, B and C; Okushima et al. (2005); Finet et al. (2013)]. Other previously identified ARF-interacting proteins have been shown to interact with the PB1 domain (Ripoll et al., 2015; Shin et al., 2007; Varaud et al., 2011) or middle region (Wu et al., 2015), which would likely modulate transcription activity. Instead, interaction of GBFs with the DBD could modify DNA-binding properties, either by exclusion or by cooperativity. GBF-binding motifs, Gboxes, were often found in close proximity to AuxREs (Berendzen et al., 2012; Cherenkov et al., 2018; Ulmasov et al., 1995), suggesting that GBFs and ARFs could regulate gene expression together. We show that the Gboxes in several vascular promoters affect the stability of expression levels in the vascular bundles and that GBF2 is able to prevent the effect of MPΔPB1 on several target genes. Thus, GBF1/2 is able to modulate and/or stabilize auxin-dependent regulation of vascular gene expression.

GBF1/2 is a strong candidate for being part of the GRN that controls the initiation of vascular identity specification. A *gfb1 gbf2 gbf3* triple mutant could not be recovered, and its potential lethality highlights a common theme in investigating the regulation of basic cell identities. Further genetic analysis, e.g. using conditional mutant alleles, could help to define the role of these transcription factors in vascular tissue initiation. The broad expression of GBFs could suggest that, similar to MP (Möller et al., 2017), their predicted cell-specific activity is influenced by local signals, such as redox potential and phosphorylation (Shaikhali et al., 2012; Klimczak et al., 1992; Smykowski et al., 2016). In a larger GRN controlling vascular identity, GBF1/2 could contribute to limiting vascular identity to the innermost cells of the early embryo. Future research into these candidate regulators is needed to confirm such a role for GBF1/2.

In conclusion, our work identifies embryonic vascular tissue identity as a primordial state from which vascular cell types evolve in diverse patterns. We find that auxin response is necessary but not sufficient for specifying this initial vascular identity. We identify a range of potential regulators of vascular identity specification and suggest a complex GRN being in control of vascular identity regulation. One potential regulator, GBF1/2, could interact with MP to modulate vascular gene expression. We expect that further analysis of these and other candidate regulators will help identify the elusive mechanism that specifies vascular tissue identity.

Development (2020) 147, dev186130. doi:10.1242/dev.186130

MATERIALS AND METHODS

Plant material and growth conditions

All *Arabidopsis* plants used in this study were of the Col-0 ecotype, except for the cell cultures, which were Landsberg *erecta*. Reporter lines for *DOF6* and *TMO6* have previously been published (Miyashima et al., 2019). Transcriptional reporters for targets of MP, *IQD15*, *SOK1*, *T5L1*, *TMO5* and *WRKY17*, have previously been published (Möller et al., 2017; Schlereth et al., 2010). The reporters for *ATHB8* and *SHR* have previously been published (Donner et al., 2009; Long et al., 2015). New reporters were generated for *WOL* and *ZLL* using the primers documented in Table S5; these reproduce previously described expression patterns (Mähönen et al., 2000; Radoeva et al., 2016). All newly generated transcriptional and translational reporter constructs (see below) were transformed into the *Arabidopsis* Col-0 wild-type accession. Misexpression lines were generated by introducing *UAS-gene* constructs into a background containing the *pRPS5A-GAL4* driver or by introducing *35S*-driven constructs into the Col-0 background. T-DNA insertion lines *gbf1* (SALK_027691), *gbf2-1* (SALK_206654), *gbf2-2* (SALK_205706) and *gbf3* (SALK_067963) were obtained from the Nottingham *Arabidopsis* Stock Centre (Nottingham, UK) and the *Arabidopsis* Biological Resource Centre (OH, USA). Plants were genotyped using the primers listed in Table S5. *Arabidopsis* seeds were surface sterilized, plated on half-strength Murashige and Skoog medium with the appropriate antibiotic (50 mg/l kanamycin or 15 mg/l phosphinothricin) and underwent 2 days of stratification at 4°C before being placed in the growth chamber. Plants were grown at 22°C under standard long-day conditions [16 h light 110 µE m^{-2} s^{-1} (Philips Master TL-D HF 50W/840) and 8 h dark].

Plant growth methods

Wild-type *Arabidopsis* Landsberg *erecta* and transgenic PSB-D cell suspension cultures were maintained in Musharige and Skoog minimal organic medium in the dark at 25°C with gentle shaking at 130 rpm. Cells were subcultured every 7 days in a 1:10 dilution with fresh medium. Transformations were conducted without callus selection, as described by Van Leene et al. (2007).

BiFC was performed by infiltrating *Nicotiana benthamiana* leaves with *Agrobacterium tumefaciens* strains carrying the appropriate plasmids (see below). Two days after infiltration, leaf sections were cut and imaged by confocal microscopy.

Protoplasts were harvested with a tape sandwich (Wu et al., 2009) and transfection was performed as described by Russinova et al. (2004). Protoplasts were prepared from plants containing a stable vascular transcriptional reporter. Green fluorescence levels were measured in protoplasts with both red (mScarlet-I) and blue (mTurquoise) fluorescence 2 days after transfection using confocal microscopy.

Vector construction for plant transformation

All constructs for plant transformation were cloned using seamless ligation cloning extract (SliCE) cloning into previously published ligation-independent cloning vectors (Wendrich et al., 2015; Zhang et al., 2014). Promoters for transcriptional reporters were introduced into the pPLV04_v2 backbone (De Rybel et al., 2011). Translational fusion constructs were generated by amplifying up to 3 kb of the promoter and the gene up to but not including the stop codon and introducing this sequence into pPLV16_v2. *UAS-gene-SRDX* overexpression constructs were cloned by introducing the amplified cDNA sequence without stop codon into a modified pPLV32_v2 backbone containing a SRDX peptide using SLiCE cloning (Wendrich et al., 2015; Zhang et al., 2014). *35S* overexpression constructs were generated by introducing the cDNA sequence into a modified pPLV26 containing a C-terminal YFP. All constructs were introduced using the simplified floral dip method as described by De Rybel et al. (2011). BiFC constructs were generated by introducing amplified cDNA sequences into modified pPLV26 vectors containing NtYFP or CtYFP, either before or after the insertion site. Binary vectors for misexpression in protoplasts were generated by introducing the cDNA of GBF2 or MPΔPB1 (first 766 amino acids) into pMON99 containing C-terminal mTurquoise or mScarlet-I. All primers used for cloning are listed in Table S5.

Microscopy

Confocal imaging was performed on a Leica SP5 II system equipped with hybrid detectors. Confocal microscopy was performed as described previously (Llavata-Peris et al., 2013). Cell walls were visualized by staining with propidium iodide (PI, for roots) or SCRI Renaissance Stain 2200 (Renaissance Chemicals R2200, for embryos).

Yeast one-hybrid

eY1H assays were performed as described previously (Gaudinier et al., 2017). The promoter used for the yeast reporter constructs (pMW2 and pMW3) was the same as the promoter used for reporting localization in *Arabidopsis*. The prey collection used was the complete *Arabidopsis* transcription factor collection available at the Brady lab (University of California, CA, USA) in July 2016 (Table S1). Network analysis was performed in Cytoscape (Shannon et al., 2003).

Affinity purification mass spectrometry sample preparation

For affinity purification, either 4 g root material or 50 ml of 3-day-old transgenic PSB-D cell suspension cultures were used, and protein extraction, pull down and sample preparation was performed as described previously (Wendrich et al., 2017). Peptides were applied to online nano LCMS/MS (Thermo Scientific) using a 60 min acetonitrile gradient from 5 to 50%. Spectra were recorded on a LTQ-XL mass spectrometer (Thermo Scientific) and analysed as described previously (Wendrich et al., 2017). Maxquant output proteingroups.txt was filtered in Perseus v. 1.6.2.3. Volcano plots were generated in R and further visualized in Adobe Illustrator.

Motif analysis

Analysis of potential binding sites presence was performed with position weight matrices taken from the Plant Transcription Factor Database (Jin et al., 2017) for GBF3 (MP00318), bZip16 (MP00291) and bZip68 (MP00173). Colocalization of binding sites with ARF-binding sites was analyzed with the MCOT package (Levitsky et al., 2019) using data on ARF2 (GSM1925138 and GSM1925826) and ARF5 (GSM1925827) binding regions from DAP-seq analysis (O'Malley et al., 2016).

ChIP-qPCR

ChIP-qPCR was performed on *Arabidopsis* cell cultures using a protocol adapted from Gendrel et al. (2005). Filtered cell culture material (3-4 g) was used as input material. After crosslinking and DNA fragmentation, the sample was split and GFP-Trap beads (Chromotek) were used to pull down GBF-YFP complexes, whereas Myc-Trap beads (Chromotek) were used for the negative control sample. qRT-PCR was performed using primers listed in Table S5. Ct values were then used to calculate fold enrichment and relative fold enrichment compared with the control regions.

Acknowledgements

The authors are grateful to Branimir Velinov, Koyan Bruggeling, Surabissree Merialu Diwakar, Sebastien Paque, Frederique Polder, Allison Gaudinier, Anne-Maarit Bagman, Joel Rodriguez-Medina, Pawel Roszak, Michelle Tang and Peter Etchells for help with experiments; to Weijers lab members for helpful discussion; and to Camila Lopez-Anido for comments on the manuscript.

Competing interests

The authors declare no competing or financial interests.

Author contributions

Conceptualization: M.E.S., D.W.; Methodology: V.L.; Validation: M.S.; Formal analysis: M.E.S., V.L., D.W.; Investigation: M.E.S., C.L-P., M.R., H.v., D.N., V.L.; Resources: I.S., P.R., D.S., G.J., S.M.B.; Writing - original draft: M.E.S., D.W.; Writing - review & editing: M.E.S., C.L.-P., M.R., H.v., D.N., V.L., D.S., G.J., V.M., S.M.B., D.W.; Visualization: M.E.S.; Supervision: G.J., V.M., S.M.B., D.W.; Project administration: D.W.; Funding acquisition: M.E.S., V.M., D.W.

Funding

This work was supported by grants from the Nederlandse Organisatie voor Wetenschappelijk Onderzoek (NWO; 831.14.003 to M.E.S. and VICI 865.14.001 to D.W.); the European Molecular Biology Organization (EMBO ASTF-368-2016 to M.E.S.); the Russian Foundation for Basic Research (19-44-543006 to D.N.); a

Wageningen Graduate Schools Sandwich PhD Scholarship (to D.N.); and Budget Project from the Russian Government (0324-2019-0040-C-01 to V.M., V.L. and D.N.). S.M.B. is a Howard Hughes Medical Institute faculty scholar.

Supplementary information

Supplementary information available online at
http://dev.biologists.org/lookup/doi/10.1242/dev.186130.supplemental

Peer review history

The peer review history is available online at https://dev.biologists.org/lookup/doi/10.1242/dev.186130.reviewer-comments.pdf

References

Abe, M., Katsumata, H., Komeda, Y. and Takahashi, T. (2003). Regulation of shoot epidermal cell differentiation by a pair of homeodomain proteins in Arabidopsis. *Development* **130**, 635-643. doi:10.1242/dev.00292

Aida, M., Ishida, T., Fukaki, H., Fujisawa, H. and Tasaka, M. (1997). Genes involved in organ separation in Arabidopsis: an analysis of the cup-shaped cotyledon mutant. *Plant Cell* **9**, 841-857. doi:10.1105/tpc.9.6.841

Baima, S., Possenti, M., Matteucci, A., Wisman, E., Altamura, M. M., Ruberti, I. and Morelli, G. (2001). The arabidopsis ATHB-8 HD-Zip protein acts as a differentiation-promoting transcription factor of the vascular meristems. *Plant Physiol.* **126**, 643-655. doi:10.1104/pp.126.2.643

Belmonte, M. F., Kirkbride, R. C., Stone, S. L., Pelletier, J. M., Bui, A. Q., Yeung, E. C., Hashimoto, M., Fei, J., Harada, C. M., Munoz, M. D. et al. (2013). Comprehensive developmental profiles of gene activity in regions and subregions of the Arabidopsis seed. *Proc. Natl. Acad. Sci. USA* **110**, E435-E444. doi:10.1073/pnas.1222061110

Bennett, M. J., Marchant, A., Green, H. G., May, S. T., Ward, S. P., Millner, P. A., Walker, A. R., Schulz, B. and Feldmann, K. A. (1996). Arabidopsis AUX1 gene: a permease-like regulator of root gravitropism. *Science* **273**, 948-950. doi:10.1126/science.273.5277.948

Berendzen, K. W., Weiste, C., Wanke, D., Kilian, J., Harter, K., Dröge-Laser, W. and Dröge-Laser, W. (2012). Bioinformatic cis-element analyses performed in Arabidopsis and rice disclose bZIP- and MYB-related binding sites as potential AuxRE-coupling elements in auxin-mediated transcription. *BMC Plant Biol.* **12**, 125. doi:10.1186/1471-2229-12-125

Berleth, T. and Jürgens, G. (1993). The role of the monopteros gene in organising the basal body region of the Arabidopsis embryo. *Development* **118**, 575-587.

Bernhardt, C., Zhao, M., Gonzalez, A., Lloyd, A. and Schiefelbein, J. (2005). The bHLH genes GL3 and EGL3 participate in an intercellular regulatory circuit that controls cell patterning in the Arabidopsis root epidermis. *Development* **132**, 291-298. doi:10.3410/f.1022891.261700

Bishopp, A., Help, H., El-Showk, S., Weijers, D., Scheres, B., Friml, J., Benková, E., Mähönen, A. P. and Helariutta, Y. (2011). A mutually inhibitory interaction between auxin and cytokinin specifies vascular pattern in roots. *Curr. Biol.* **21**, 917-926. doi:10.1016/j.cub.2011.04.017

Blob, B., Heo, J. and Helariutta, Y. (2018). Phloem differentiation: an integrative model for cell specification. *J. Plant Res.* **131**, 31-36. doi:10.1007/s10265-017-0999-0

Bonke, M., Thitamadee, S., Mähönen, A. P., Hauser, M.-T. and Helariutta, Y. (2003). APL regulates vascular tissue identity in Arabidopsis. *Nature* **426**, 181-186. doi:10.1038/nature02100

Brackmann, K., Qi, J., Gebert, M., Jouannet, V., Schlamp, T., Grünwald, K., Wallner, E.-S., Novikova, D. D., Levitsky, V. G., Agustí, J. et al. (2018). Spatial specificity of auxin responses coordinates wood formation. *Nat. Commun.* **9**, 875. doi:10.1038/s41467-018-03256-2

Brady, S. M., Orlando, D. A., Lee, J.-Y., Wang, J. Y., Koch, J., Dinneny, J. R., Mace, D., Ohler, U. and Benfey, P. N. (2007). A high-resolution root spatiotemporal map reveals dominant expression patterns. *Science* **318**, 801-806. doi:10.1126/science.1146265

Carlsbecker, A., Lee, J.-Y., Roberts, C. J., Dettmer, J., Lehesranta, S., Zhou, J., Lindgren, O., Moreno-Risueno, M. A., Vatén, A., Thitamadee, S. et al. (2010). Cell signalling by microRNA165/6 directs gene dose-dependent root cell fate. *Nature* **465**, 316-321. doi:10.1038/nature08977

Cheng, Y., Dai, X. and Zhao, Y. (2006). Auxin biosynthesis by the YUCCA flavin monooxygenases controls the formation of floral organs and vascular tissues in Arabidopsis. *Genes Dev.* **20**, 1790-1799. doi:10.1101/gad.1415106

Cherenkov, P., Novikova, D., Omelyanchuk, N., Levitsky, V., Grosse, I., Weijers, D. and Mironova, V. (2018). Diversity of cis-regulatory elements associated with auxin response in Arabidopsis thaliana. *J. Exp. Bot.* **69**, 329-339. doi:10.1093/jxb/erx254

Curaba, J., Herzog, M. and Vachon, G. (2003). GeBP, the first member of a new gene family in Arabidopsis, encodes a nuclear protein with DNA-binding activity and is regulated by KNAT1. *Plant J.* **33**, 305-317. doi:10.1046/j.1365-313X.2003.01622.x

De Rybel, B., Van Den Berg, W., Lokerse, A. S., Liao, C.-Y., Van Mourik, H., Möller, B., Llavata-Peris, C. I. and Weijers, D. (2011). A versatile set of ligation-independent cloning vectors for functional studies in plants. *Plant Physiol.* **156**, 1292-1299. doi:10.1104/pp.111.177337

De Rybel, B., Möller, B., Yoshida, S., Grabowicz, I., Barbier de Reuille, P., Boeren, S., Smith, R. S., Borst, J. W. and Weijers, D. (2013). A bHLH complex controls embryonic vascular tissue establishment and indeterminate growth in arabidopsis. *Dev. Cell* **24**, 426-437. doi:10.1016/j.devcel.2012.12.013

De Rybel, B., Adibi, M., Breda, A. S., Wendrich, J. R., Smit, M. E., Novak, O., Yamaguchi, N., Yoshida, S., Van Isterdael, G., Palovaara, J. et al. (2014). Integration of growth and patterning during vascular tissue formation in Arabidopsis. *Science* **345**, 1255215. doi:10.1126/science.1255215

Denyer, T., Ma, X., Klesen, S., Scacchi, E., Nieselt, K. and Timmermans, M. C. P. (2019). Spatiotemporal developmental trajectories in the arabidopsis root revealed using high-throughput single-cell RNA sequencing. *Dev. Cell* **48**, 840-852.e5. doi:10.1016/j.devcel.2019.02.022

Donner, T. J., Sherr, I. and Scarpella, E. (2009). Regulation of preprocambial cell state acquisition by auxin signaling in Arabidopsis leaves. *Development* **136**, 3235-3246. doi:10.1242/dev.037028

Dröge-Laser, W., Snoek, B. L., Snel, B. and Weiste, C. (2018). The Arabidopsis bZIP transcription factor family — an update. *Curr. Opin. Plant Biol.* **45**, 36-49. doi:10.1016/j.pbi.2018.05.001

Etchells, J. P., Provost, C. M., Mishra, L. and Turner, S. R. (2013). WOX4 and WOX14 act downstream of the PXY receptor kinase to regulate plant vascular proliferation independently of any role in vascular organisation. *Development* **140**, 2224-2234. doi:10.1242/dev.091314

Finet, C., Berne-Dedieu, A., Scutt, C. P. and Marlétaz, F. (2013). Evolution of the ARF gene family in land plants: old domains, new tricks. *Mol. Biol. Evol.* **30**, 45-56. doi:10.1093/molbev/mss220

Fisher, K. and Turner, S. (2007). PXY, a receptor-like kinase essential for maintaining polarity during plant vascular-tissue development. *Curr. Biol.* **17**, 1061-1066. doi:10.1016/j.cub.2007.05.049

Gardiner, J., Donner, T. J. and Scarpella, E. (2011). Simultaneous activation of SHR and ATHB8 expression defines switch to preprocambial cell state in Arabidopsis leaf development. *Dev. Dyn.* **240**, 261-270. doi:10.1002/dvdy.22516

Gaudinier, A., Zhang, L., Reece-Hoyes, J. S., Taylor-Teeples, M., Pu, L., Liu, Z., Breton, G., Pruneda-Paz, J. L., Kim, D., Kay, S. A. et al. (2011). Enhanced Y1H assays for Arabidopsis. *Nat. Methods* **8**, 1053-1055. doi:10.1038/nmeth.1750

Gaudinier, A., Tang, M., Bågman, A.-M. and Brady, S. M. (2017). Identification of protein–DNA interactions using enhanced yeast one-hybrid assays and a semiautomated approach. *Methods Mol. Biol.* **1610**, 187-215. doi:10.1007/978-1-4939-7003-2_13

Gaudinier, A., Rodriguez-Medina, J., Zhang, L., Olson, A., Liseron-Monfils, C., Bågman, A.-M., Foret, J., Abbitt, S., Tang, M., Li, B. et al. (2018). Transcriptional regulation of nitrogen-associated metabolism and growth. *Nature* **563**, 259-264. doi:10.1038/s41586-018-0656-3

Gendrel, A.-V., Lippman, Z., Martienssen, R. and Colot, V. (2005). Profiling histone modification patterns in plants using genomic tiling microarrays. *Nat. Methods* **2**, 213-218. doi:10.1038/nmeth0305-213

Giri, M. K., Singh, N., Banday, Z. Z., Singh, V., Ram, H., Singh, D., Chattopadhyay, S. and Nandi, A. K. (2017). GBF1 differentially regulates CAT2 and PAD4 transcription to promote pathogen defense in Arabidopsis thaliana. *Plant J.* **91**, 802-815. doi:10.1111/tpj.13608

Hamann, T., Mayer, U. and Jürgens, G. (1999). The auxin-insensitive bodenlos mutation affects primary root formation and apical-basal patterning in the Arabidopsis embryo. *Development* **126**, 1387-1395.

Hamann, T., Benkova, E., Bäurle, I., Kientz, M. and Jürgens, G. (2002). The Arabidopsis BODENLOS gene encodes an auxin response protein inhibiting MONOPTEROS-mediated embryo patterning. *Genes Dev.* **16**, 1610-1615. doi:10.1101/gad.229402

Han, S., Cho, H., Noh, J., Qi, J., Jung, H.-J., Nam, H., Lee, S., Hwang, D., Greb, T. and Hwang, I. (2018). BIL1mediated MP phosphorylation integrates PXY and cytokinin signalling in secondary growth. *Nat. Plants* **4**, 605-614. doi:10.1038/s41477-018-0180-3

Hardtke, C. S. and Berleth, T. (1998). The Arabidopsis gene MONOPTEROS encodes a transcription factor mediating embryo axis formation and vascular development. *EMBO J.* **17**, 1405-1411. doi:10.1093/emboj/17.5.1405

Haseloff, J. (1999). GFP variants for multispectral imaging of living cells. *Methods Cell Biol.* **58**, 139-151. doi:10.1016/S0091-679X(08)61953-6

Hirakawa, Y., Kondo, Y. and Fukuda, H. (2010). TDIF peptide signaling regulates vascular stem cell proliferation via the WOX4 homeobox gene in Arabidopsis. *Plant Cell* **22**, 2618-2629. doi:10.1105/tpc.110.076083

Hu, C.-D., Chinenov, Y. and Kerppola, T. K. (2002). Visualization of interactions among bZIP and Rel family proteins in living cells using bimolecular fluorescence complementation. *Mol. Cell.* **9**, 789-798. doi:10.1016/S1097-2765(02)00496-3

Jacobs, W. P. (1952). The role of Auxin in differentiation of xylem around a wound. *Am. J. Bot.* **39**, 301. doi:10.1002/j.1537-2197.1952.tb14277.x

Jakoby, M., Weisshaar, B., Dröge-Laser, W., Vicente-Carbajosa, J., Tiedemann, J., Kroj, T., Parcy, F. and bZIP Research Group. (2002). bZIP transcription factors in Arabidopsis. *Trends Plant Sci.* **7**, 106-111. doi:10.1016/S1360-1385(01)02223-3

Jin, J., Tian, F., Yang, D.-C., Meng, Y.-Q., Kong, L., Luo, J. and Gao, G. (2017). PlantTFDB 4.0: toward a central hub for transcription factors and regulatory interactions in plants. *Nucleic Acids Res.* **45**, D1040-D1045. doi:10.1093/nar/gkw982

Kirch, T., Simon, R., Grünewald, M. and Werr, W. (2003). The Dornröschen/enhancer of shoot regeneration1: gene of Arabidopsis acts in the control of meristem cell fate and lateral organ development. *Plant Cell* **15**, 694-705. doi:10.1105/tpc.009480

Klimczak, L. J., Schindler, U. and Cashmore, A. R. (1992). DNA binding activity of the Arabidopsis G-box binding factor GBF1 is stimulated by phosphorylation by casein kinase II from Broccoli. *Plant Cell* **4**, 87-98. doi:10.1105/tpc.4.1.87

Kondo, Y., Fujita, T., Sugiyama, M. and Fukuda, H. (2015). A novel system for xylem cell differentiation in arabidopsis thaliana. *Mol. Plant* **8**, 612-621. doi:10.1016/j.molp.2014.10.008

Krogan, N. T., Ckurshumova, W., Marcos, D., Caragea, A. E. and Berleth, T. (2012). Deletion of MP/ARF5 domains III and IV reveals a requirement for Aux/IAA regulation in Arabidopsis leaf vascular patterning. *New Phytol.* **194**, 391-401. doi:10.1111/j.1469-8137.2012.04064.x

Kubo, M., Udagawa, M., Nishikubo, N., Horiguchi, G., Yamaguchi, M., Ito, J., Mimura, T., Fukuda, H. and Demura, T. (2005). Transcription switches for protoxylem and metaxylem vessel formation. *Genes Dev.* **19**, 1855-1860. doi:10.1101/gad.1331305

Lau, O. S., Davies, K. A., Chang, J., Adrian, J., Rowe, M. H., Ballenger, C. E. and Bergmann, D. C. (2014). Direct roles of SPEECHLESS in the specification of stomatal self-renewing cells. *Science* **345**, 1605-1609. doi:10.1126/science.1256888

Lee, M. M. and Schiefelbein, J. (1999). WEREWOLF, a MYB-related protein in Arabidopsis, is a positiondependent regulator of epidermal cell patterning. *Cell* **99**, 473-483. doi:10.1016/S0092-8674(00)81536-6

Lee, J.-Y., Colinas, J., Wang, J. Y., Mace, D., Ohler, U. and Benfey, P. N. (2006). Transcriptional and posttranscriptional regulation of transcription factor expression in Arabidopsis roots. *Proc. Natl. Acad. Sci. USA* **103**, 6055-6060. doi:10.1073/pnas.0510607103

León, J., Rojo, E. and Sánchez-Serrano, J. J. (2001). Wound signalling in plants. *J. Exp. Bot.* **52**, 1-9. doi:10.1093/jxb/52.354.1

Levitsky, V., Zemlyanskaya, E., Oshchepkov, D., Podkolodnaya, O., Ignatieva, E., Grosse, I., Mironova, V. and Merkulova, T. (2019). A single ChIP-seq dataset is sufficient for comprehensive analysis of motifs cooccurrence with MCOT package. *Nucleic Acids Res.* **47**, e139. doi:10.1093/nar/gkz800

Lian, T.-F., Xu, Y.-P., Li, L.-F. and Su, X.-D. (2017). Crystal structure of Tetrameric Arabidopsis MYC2 reveals the mechanism of enhanced interaction with DNA. *Cell Rep.* **19**, 1334-1342. doi:10.1016/j.celrep.2017.04.057

Liao, C.-Y., Smet, W., Brunoud, G., Yoshida, S., Vernoux, T. and Weijers, D. (2015). Reporters for sensitive and quantitative measurement of auxin response. *Nat. Methods* **12**, 207-210. doi:10.1038/nmeth.3279

Llavata-Peris, C., Lokerse, A., Möller, B., De Rybel, B. and Weijers, D. (2013). Imaging of phenotypes, gene expression, and protein localization during embryonic root formation in arabidopsis. *Methods Mol. Biol.* **959**, 137-148. doi:10.1007/978-1-62703-221-6_8

Long, Y., Smet, W., Cruz-Ramírez, A., Castelijns, B., De Jonge, W., Mähönen, A. P., Bouchet, B. P., Perez, G. S., Akhmanova, A., Scheres, B., et al. (2015). Arabidopsis BIRD Zinc finger proteins jointly stabilize tissue boundaries by confining the cell fate regulator SHORT-ROOT and contributing to fate specification. *Plant Cell* **27**, 1185-1199. doi:10.1105/tpc.114.132407

Mähönen, A. P., Bonke, M., Kauppinen, L., Riikonen, M., Benfey, P. N. and Helariutta, Y. (2000). A novel two-component hybrid molecule regulates vascular morphogenesis of the Arabidopsis root. *Genes Dev.* **14**, 2938-2943. doi:10.1101/gad.189200

Mähönen, A. P., Bishopp, A., Higuchi, M., Nieminen, K. M., Kinoshita, K., Törmäkangas, K., Ikeda, Y., Oka, A., Kakimoto, T. and Helariutta, Y. (2006). Cytokinin signaling and its inhibitor AHP6 regulate cell fate during vascular development. *Science* **311**, 94-98. doi:10.1126/science.1118875

Mallappa, C., Yadav, V., Negi, P. and Chattopadhyay, S. (2006). A basic leucine zipper transcription factor, G-box-binding factor 1, regulates blue light-mediated photomorphogenic growth in Arabidopsis. *J. Biol. Chem.* **281**, 22190-22199. doi:10.1074/jbc.M601172200

Marchant, A. (1999). AUX1 regulates root gravitropism in Arabidopsis by facilitating auxin uptake within root apical tissues. *EMBO J.* **18**, 2066-2073. doi:10.1093/emboj/18.8.2066

Mattsson, J., Ckurshumova, W. and Berleth, T. (2003). Auxin signaling in Arabidopsis leaf vascular development. *Plant Physiol.* **131**, 1327-1339. doi:10.1104/pp.013623

Mayer, U., Ruiz, R. A. T., Berleth, T., Miséra, S. and Jürgens, G. (1991). Mutations affecting body organization in the Arabidopsis embryo. *Nature* **353**, 402-407. doi:10.1038/353402a0

McCarthy, R. L., Zhong, R. and Ye, Z.-H. (2009). MYB83 is a direct target of SND1 and acts redundantly with MYB46 in the regulation of secondary cell wall biosynthesis in arabidopsis. *Plant Cell Physiol.* **50**, 1950-1964. doi:10.1093/pcp/pcp139

McConnell, J. R., Emery, J., Eshed, Y., Bao, N., Bowman, J. and Barton, M. K. (2001). Role of PHABULOSA and PHAVOLUTA in determining radial patterning in shoots. *Nature* **411**, 709-713. doi:10.1038/35079635

Melnyk, C. W., Schuster, C., Leyser, O. and Meyerowitz, E. M. (2015). A developmental framework for graft formation and vascular reconnection in arabidopsis thaliana. *Curr. Biol.* **25**, 1306-1318. doi:10.1016/j.cub.2015.03.032

Melnyk, C. W., Gabel, A., Hardcastle, T. J., Robinson, S., Miyashima, S., Grosse, I. and Meyerowitz, E. M. (2018). Transcriptome dynamics at Arabidopsis graft junctions reveal an intertissue recognition mechanism that activates vascular regeneration. *Proc. Natl. Acad. Sci. USA* **115**, E2447-E2456. doi:10.1073/pnas.1718263115

Miyashima, S., Roszak, P., Sevilem, I., Toyokura, K., Blob, B., Heo, J.-., Mellor, N., Help-Rinta-Rahko, H., Otero, S., Smet, W. et al. (2019). Mobile PEAR transcription factors integrate positional cues to prime cambial growth. *Nature* **565**, 490-494. doi:10.1038/s41586-018-0839-y

Möller, B. K., Ten Hove, C. A., Xiang, D., Williams, N., López, L. G., Yoshida, S., Smit, M., Datla, R. and Weijers, D. (2017). Auxin response cell-autonomously controls ground tissue initiation in the early *Arabidopsis* embryo. *Proc. Natl. Acad. Sci. USA* **114**, E2533-E2539. doi:10.1073/pnas.1616493114

Nanao, M. H., Vinos-Poyo, T., Brunoud, G., Thévenon, E., Mazzoleni, M., Mast, D., Lainé, S., Wang, S., Hagen, G., Li, H. et al. (2014). Structural basis for oligomerization of auxin transcriptional regulators. *Nat. Commun.* **5**, 3617. doi:10.1038/ncomms4617

Ohashi-Ito, K., Matsukawa, M. and Fukuda, H. (2013). An atypical bHLH transcription factor regulates early xylem development downstream of auxin. *Plant Cell Physiol.* **54**, 398-405. doi:10.1093/pcp/pct013

Ohashi-Ito, K., Saegusa, M., Iwamoto, K., Oda, Y., Katayama, H., Kojima, M., Sakakibara, H. and Fukuda, H. (2014). A bHLH complex activates vascular cell division via cytokinin action in root apical meristem. *Curr. Biol.* **24**, 2053-2058. doi:10.1016/j.cub.2014.07.050

Ohno, C. K., Reddy, G. V., Heisler, M. G. B. and Meyerowitz, E. M. (2004). The Arabidopsis JAGGED gene encodes a zinc finger protein that promotes leaf tissue development. *Development* **131**, 1111-1122. doi:10.1242/dev.00991

Okushima, Y., Overvoorde, P. J., Arima, K., Alonso, J. M., Chan, A., Chang, C., Ecker, J. R., Hughes, B., Lui, A., Nguyen, D. et al. (2005). Functional genomic analysis of the AUXIN RESPONSE FACTOR gene family members in Arabidopsis thaliana: unique and overlapping functions of ARF7 and ARF19. *Plant Cell* **17**, 444-463. doi:10.1105/tpc.104.028316

O'Malley, R. C., Huang, S.-S. C., Song, L., Lewsey, M. G., Bartlett, A., Nery, J. R., Galli, M., Gallavotti, A. and Ecker, J. R. (2016). Cistrome and Epicistrome features shape the regulatory DNA landscape. *Cell* **165**, 1280-1292. doi:10.1016/j.cell.2016.04.038

Palovaara, J., Saiga, S., Wendrich, J. R., Van 'T Wout Hofland, N., Van Schayck, J. P., Hater, F., Mutte, S., Sjollema, J., Boekschoten, M., Hooiveld, G. J., et al. (2017). Transcriptome dynamics revealed by a gene expression atlas of the early Arabidopsis embryo. *Nat. Plants* **3**, 894-904. doi:10.1038/s41477-017-0035-3

Przemeck, G. K. H., Mattsson, J., Hardtke, C. S., Sung, Z. R. and Berleth, T. (1996). Studies on the role of the Arabidopsis gene MONOPTEROS in vascular development and plant cell axialization. *Planta* **200**, 229-237. doi:10.1007/BF00208313

Rademacher, E. H., Lokerse, A. S., Schlereth, A., Llavata-Peris, C. I., Bayer, M., Kientz, M., Freire Rios, A., Borst, J. W., Lukowitz, W., Jürgens, G., et al. (2012). Different auxin response machineries control distinct cell fates in the early plant embryo. *Dev. Cell* **22**, 211-222. doi:10.1016/j.devcel.2011.10.026

Radoeva, T., Ten Hove, C. A., Saiga, S. and Weijers, D. (2016). Molecular characterization of arabidopsis GAL4/UAS enhancer trap lines identifies novel cell type-specific promoters. *Plant Physiol.* **171**, 1169-1181. doi:10.1104/pp.16.00213

Reece-Hoyes, J. S., Diallo, A., Lajoie, B., Kent, A., Shrestha, S., Kadreppa, S., Pesyna, C., Dekker, J., Myers, C. L. and Walhout, A. J. M. (2011). Enhanced yeast one-hybrid assays for high-throughput gene-centered regulatory network mapping. *Nat. Methods* **8**, 1059-1064. doi:10.1038/nmeth.1748

Ripoll, J. J., Bailey, L. J., Mai, Q.-A., Wu, S. L., Hon, C. T., Chapman, E. J., Ditta, G. S., Estelle, M. and Yanofsky, M. F. (2015). microRNA regulation of fruit growth. *Nat. Plants* **1**, 15036. doi:10.1038/nplants.2015.36

Rodriguez-Villalon, A., Gujas, B., Kang, Y. H., Breda, A. S., Cattaneo, P., Depuydt, S. and Hardtke, C. S. (2014). Molecular genetic framework for protophloem formation. *Proc. Natl. Acad. Sci. USA* **111**, 11551-11556. doi:10.1073/pnas.1407337111

Ruiz Sola, M. A., Coiro, M., Crivelli, S., Zeeman, S. C., Schmidt Kjølner Hansen, S. and Truernit, E. (2017). OCTOPUS-LIKE 2, a novel player in Arabidopsis root and vascular development, reveals a key role for OCTOPUS family genes in root metaphloem sieve tube differentiation. *New Phytol.* **216**, 1191-1204. doi:10.1111/nph.14751

Russinova, E., Borst, J.-W., Kwaaitaal, M., Caño-Delgado, A., Yin, Y., Chory, J. and De Vries, S. C. (2004). Heterodimerization and endocytosis of Arabidopsis brassinosteroid receptors BRI1 and AtSERK3 (BAK1). *Plant Cell* **16**, 3216-3229. doi:10.1105/tpc.104.025387

Ryu, K. H., Huang, L., Kang, H. M. and Schiefelbein, J. (2019). Single-cell RNA sequencing resolves molecular relationships among individual plant cells. *Plant Physiol.* **179**, 1444-1456. doi:10.1104/pp.18.01482

Sachs, T. (1969). Polarity and the induction of organized vascular tissues. *Ann. Bot.* **33**, 263-275. doi:10.1093/oxfordjournals.aob.a084281
Sachs, T. (1981). The control of the patterned differentiation of vascular tissues. *Adv. Bot. Res.* **9**, 151-262. doi:10.1016/S0065-2296(08)60351-1
Sakai, H., Honma, T., Takashi, A., Sato, S., Kato, T., Tabata, S. and Oka, A. (2001). ARR1, a transcription factor for genes immediately responsive to cytokinins. *Science* **294**, 1519-1521. doi:10.1126/science.1065201
Scarpella, E., Marcos, D., Friml, J. J. and Berleth, T. (2006). Control of leaf vascular patterning by polar auxin transport. *Genes Dev.* **20**, 1015-1027. doi:10.1101/gad.1402406
Scheres, B., Wolkenfelt, H., Willemsen, V., Terlouw, M., Lawson, E., Dean, C. and Weisbeek, P. (1994). Embryonic origin of the Arabidopsis primary root and root meristem initials. *Development* **120**, 2475-2487. doi:10.1007/978-3-642-78852-9_5
Scheres, B., Dilaurenzio, L., Willemsen, V., Hauser, M. T., Janmaat, K., Weisbeek, P. and Benfey, P. N. (1995). Mutations affecting the radial organisation of the Arabidopsis root display specific defects throughout the embryonic axis. *Development* **121**, 53-62.
Schindler, U., Terzaghi, W., Beckmann, H., Kadesch, T. and Cashmore, A. R. (1992). DNA binding site preferences and transcriptional activation properties of the Arabidopsis transcription factor GBF1. *EMBO J.* **11**, 1275-1289. doi:10.1002/j.1460-2075.1992.tb05171.x
Schlereth, A., Möller, B., Liu, W., Kientz, M., Flipse, J., Rademacher, E. H., Schmid, M., Jürgens, G. and Weijers, D. (2010). MONOPTEROS controls embryonic root initiation by regulating a mobile transcription factor. *Nature* **464**, 913-916. doi:10.1038/nature08836
Schon, M. A. and Nodine, M. D. (2017). Widespread contamination of arabidopsis embryo and endosperm transcriptome data sets. *Plant Cell* **29**, 608-617. doi:10.1105/tpc.16.00845
Shaikhali, J., Norén, L., De Dios Barajas-López, J., Srivastava, V., König, J., Sauer, U. H., Wingsle, G., Dietz, K.-J. and Strand, Å. (2012). Redox-mediated mechanisms regulate DNA binding activity of the G-group of basic region leucine zipper (bZIP) transcription factors in Arabidopsis. *J. Biol. Chem.* **287**, 27510-27525. doi:10.1074/jbc.M112.361394
Shannon, P., Markiel, A., Ozier, O., Baliga, N. S., Wang, J. T., Ramage, D., Amin, N., Schwikowski, B. and Ideker, T. (2003). Cytoscape: a software Environment for integrated models of biomolecular interaction networks. *Genome Res.* **13**, 2498-2504. doi:10.1101/gr.1239303
Shin, R., Burch, A. Y., Huppert, K. A., Tiwari, S. B., Murphy, A. S., Guilfoyle, T. J. and Schachtman, D. P. (2007). The arabidopsis transcription factor MYB77 modulates auxin signal transduction. *Plant Cell* **19**, 2440-2453. doi:10.1105/tpc.107.050963
Shulse, C. N., Cole, B. J., Ciobanu, D., Lin, J., Yoshinaga, Y., Gouran, M., Turco, G. M., Zhu, Y., O'Malley, R. C., Brady, S. M. et al. (2019). High-throughput single-cell transcriptome profiling of plant cell types. *Cell Rep.* **14**, 2241-2247. doi:10.1016/j.celrep.2019.04.054
Singh, A., Ram, H., Abbas, N. and Chattopadhyay, S. (2012). Molecular interactions of GBF1 with HY5 and HYH proteins during light-mediated seedling development in Arabidopsis thaliana. *J. Biol. Chem.* **287**, 25995-26009. doi:10.1074/jbc.M111.333906
Slane, D., Kong, J., Berendzen, K. W., Kilian, J., Henschen, A., Kolb, M., Schmid, M., Harter, K., Mayer, U., De Smet, I., et al. (2014). Cell type-specific transcriptome analysis in the early arabidopsis thaliana embryo. *Development* **141**, 4831-4840. doi:10.1242/dev.116459
Smetana, O., Mäkilä, R., Lyu, M., Amiryousefi, A., Sánchez Rodríguez, F., Wu, M.-F., Solé-Gil, A., Leal Gavarrón, M., Siligato, R., Miyashima, S. et al. (2019). High levels of auxin signalling define the stem-cell organizer of the vascular cambium. *Nature* **565**, 485-489. doi:10.1038/s41586-018-0837-0
Smit, M. E., McGregor, S. R., Sun, H., Gough, C., Bågman, A. M., Soyars, C. L., Kroon, J. T., Gaudinier, A., Williams, C. J., Yang, X. et al. (2020). A PXY-Mediated transcriptional network Integrates signaling mechanisms to control vascular development in Arabidopsis. *Plant Cell* **32**, 319-335. doi:10.1105/tpc.19.00562
Smykowski, A., Zimmermann, P. and Zentgraf, U. (2010). G-box binding factor1 reduces CATALASE2 expression and regulates the onset of leaf senescence in arabidopsis. *Plant Physiol.* **153**, 1321-1331. doi:10.1104/pp.110.157180
Smykowski, A., Fischer, S. and Zentgraf, U. (2016). Phosphorylation affects DNA-binding of the SenescenceRegulating bZIP transcription factor GBF1. *Plants* **4**, 691-709. doi:10.3390/plants4030691
Taylor-Teeples, M., Lin, L., De Lucas, M., Turco, G., Toal, T. W., Gaudinier, A., Young, N. F., Trabucco, G. M., Veling, M. T., Lamothe, R. et al. (2015). An Arabidopsis gene regulatory network for secondary cell wall synthesis. *Nature* **517**, 571-575. doi:10.1038/nature14099
Tucker, M. R., Hinze, A., Tucker, E. J., Takada, S., Jurgens, G. and Laux, T. (2008). Vascular signalling mediated by ZWILLE potentiates WUSCHEL function during shoot meristem stem cell development in the Arabidopsis embryo. *Development* **135**, 2839-2843. doi:10.1242/dev.023648
Ulmasov, T., Liu, Z. B., Hagen, G. and Guilfoyle, T. J. (1995). Composite structure of auxin response elements. *Plant Cell* **7**, 1611-1623. doi:10.1105/tpc.7.10.1611
Van Den Berg, T. and ten Tusscher, K. H. (2017). Auxin information processing; partners and interactions beyond the usual suspects. *Int. J. Mol. Sci.* **18**, E2585. doi:10.3390/ijms18122585
Van Leene, J., Stals, H., Eeckhout, D., Persiau, G., Van De Slijke, E., Van Isterdael, G., De Clercq, A., Bonnet, E., Laukens, K., Remmerie, N. et al. (2007). A tandem affinity purification-based technology platform to study the cell cycle interactome in Arabidopsis thaliana. *Mol. Cell. Proteomics* **6**, 1226-1238. doi:10.1074/mcp.M700078-MCP200
Varaud, E., Szécsi, J., Brioudes, F., Perrot-Rechenmann, C., Brown, S., Bendahmane, M. and Leroux, J. (2011). AUXIN RESPONSE FACTOR8 Regulates Arabidopsis Petal Growth by Interacting with the bHLH Transcription Factor BIGPETALp. *Plant Cell* **23**, 973-983. doi:10.1105/tpc.110.081653
Wabnik, K., Robert, H. S., Smith, R. S. and Friml, J. (2013). Modeling framework for the establishment of the apical-basal embryonic axis in plants. *Curr. Biol.* **23**, 2513-2518. doi:10.1016/j.cub.2013.10.038
Wallner, E.-S., López-Salmerón, V., Belevich, I., Poschet, G., Jung, I., Grünwald, K., Sevilem, I., Jokitalo, E., Hell, R., Helariutta, Y. et al. (2017). Strigolactone- and Karrikin-independent SMXL proteins are central regulators of phloem formation. *Curr. Biol.* **27**, 1241-1247. doi:10.1016/j.cub.2017.03.014
Walter, M., Chaban, C., Schütze, K., Batistic, O., Weckermann, K., Näke, C., Blazevic, D., Grefen, C., Schumacher, K., Oecking, C., et al. (2004). Visualization of protein interactions in living plant cells using bimolecular fluorescence complementation. *Plant J.* **40**, 428-438. doi:10.1111/j.1365-313X.2004.02219.x
Weijers, D., Franke-Van Dijk, M., Vencken, R. J., Quint, A., Hooykaas, P. and Offringa, R. (2001). An Arabidopsis Minute-like phenotype caused by a semi-dominant mutation in a RIBOSOMAL PROTEIN S5 gene. *Development* **128**, 4289-4299.
Weijers, D., Schlereth, A., Ehrismann, J. S., Schwank, G., Kientz, M. and Jürgens, G. (2006). Auxin triggers transient local signaling for cell specification in Arabidopsis embryogenesis. *Dev. Cell* **10**, 265-270. doi:10.1016/j.devcel.2005.12.001
Weiste, C. and Dröge-Laser, W. (2014). The Arabidopsis transcription factor bZIP11activates auxin-mediated transcription by recruiting the histone acetylation machinery. *Nat. Commun.* **5**, 3883. doi:10.1038/ncomms4883
Wendrich, J. R., Liao, C.-Y., Van Den Berg, W. A. M., De Rybel, B. and Weijers, D. (2015). Ligation-independent cloning for plant research. *Methods Mol. Biol.*, 421-431. doi:10.1007/978-1-4939-2444-8_21
Wendrich, J. R., Boeren, S., Möller, B. K., Weijers, D. and De Rybel, B. (2017). In vivo identification of plant protein complexes using IP-MS/MS. *Methods Mol. Biol.* **1284**, 147-158. doi:10.1007/978-1-4939-6469-7_14
Wetmore, R. H. and Rier, J. P. (1963). Experimental induction of vascular tissues in callus of angiosperms. *Am. J. Bot.* **50**, 418. doi:10.2307/2440311
Wu, F.-H., Shen, S.-C., Lee, L.-Y., Lee, S.-H., Chan, M.-T. and Lin, C.-S. (2009). Tape-arabidopsis sandwich - a simpler arabidopsis protoplast isolation method. *Plant Methods* **5**, 16 doi:10.1186/1746-4811-5-16
Wu, M. F., Yamaguchi, N., Xiao, J., Bargmann, B., Estelle, M., Sang, Y. and Wagner, D. (2015). Auxin-regulated chromatin switch directs acquisition of flower primordium founder fate. *eLife* **4**, e09269. doi:10.7554/eLife.09269.027
Yamaguchi, M., Goué, N., Igarashi, H., Ohtani, M., Nakano, Y., Mortimer, J. C., Nishikubo, N., Kubo, M., Katayama, Y., Kakegawa, K., et al. (2010). VASCULAR-RELATED NAC-DOMAIN6 and VASCULAR-RELATED NAC-DOMAIN7 effectively induce transdifferentiation into xylem vessel elements under control of an induction system. *Plant Physiol.* **153**, 906-914. doi:10.1104/pp.110.154013
Yang, K.-Z., Jiang, M., Wang, M., Xue, S., Zhu, L.-L., Wang, H.-Z., Zou, J.-J., Lee, E.-K., Sack, F. and Le, J. (2015). Phosphorylation of serine 186 of bHLH transcription factor SPEECHLESS promotes stomatal development in Arabidopsis. *Mol. Plant* **8**, 783-795. doi:10.1016/j.molp.2014.12.014
Yin, H., Yan, B., Sun, J., Jia, P., Zhang, Z., Yan, X., Chai, J., Ren, Z., Zheng, G. and Liu, H. (2012). Graft-union development: a delicate process that involves cell-cell communication between scion and stock for local auxin accumulation. *J. Exp. Bot.* **63**, 4219-4232. doi:10.1093/jxb/ers109
Yoshida, S., Barbier de Reuille, P., Lane, B., Bassel, G. W., Prusinkiewicz, P., Smith, R. S. and Weijers, D. (2014). Genetic control of plant development by overriding a geometric division rule. *Dev. Cell* **29**, 75-87. doi:10.1016/j.devcel.2014.02.002
Yoshida, S., Van Der Schuren, A., Van Dop, M., Van Galen, L., Saiga, S., Adibi, M., Möller, B., Ten Hove, C. A., Marhavy, P., Smith, R., et al. (2019). A SOSEKI-based coordinate system interprets global polarity cues in Arabidopsis. *Nat. Plants* **5**, 160-166. doi:10.1038/s41477-019-0363-6
Zhang, Y., Werling, U. and Edelmann, W. (2014). Seamless Ligation Cloning Extract (SLiCE) cloning method. *Methods Mol. Biol.* **1116**, 235-1244. doi:10.1007/978-1-62703-764-8_16
Zhang, Y., Guo, X. and Dong, J. (2016). Phosphorylation of the polarity protein BASL differentiates asymmetric cell fate through MAPKs and SPCH. *Curr. Biol.* **26**, 2957-2965. doi:10.1016/j.cub.2016.08.066

Figure S1

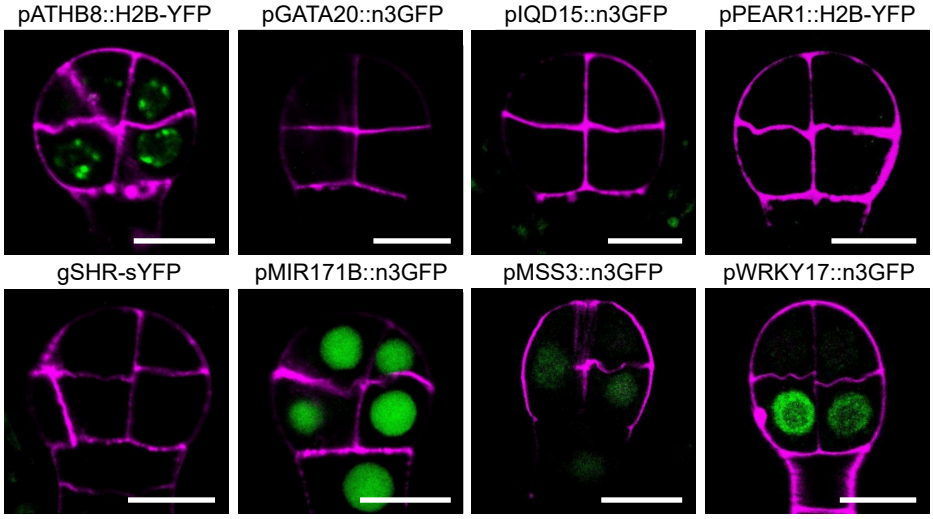

Figure S1: Expression of vascular markers in the 8-cell stage embryo. Activity of 8 vascular transcriptional reporter in the 8-cell stage embryo. Fluorescent protein signals are displayed in green, cell wall staining in magenta. Roots are stained with PI, embryos with Renaissance. Scale bars represent 10 µm.

Figure S2

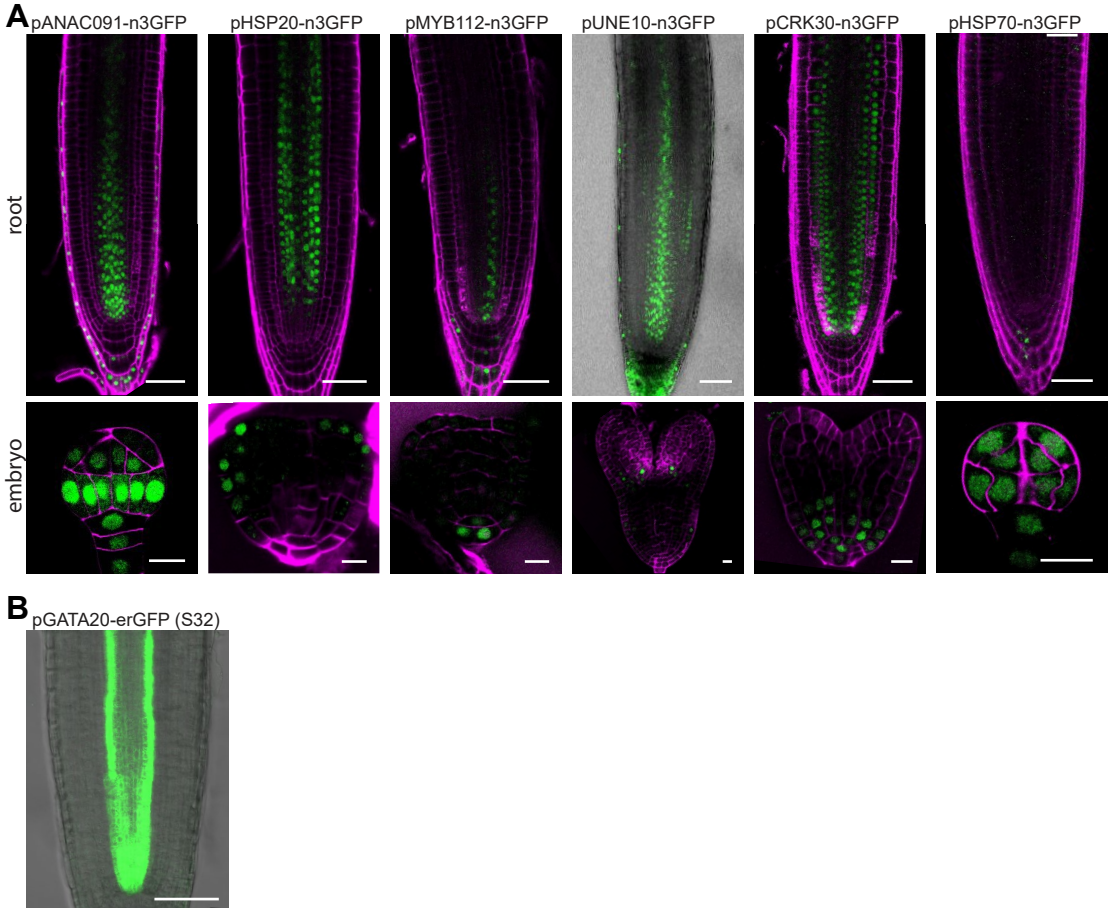

Figure S2: Diverging expression patterns between root and embryo. (A) Activity of transcriptional reporters in the root tip and embryo. Fluorescent protein signals are displayed in green, cell wall staining in magenta. Roots are stained with PI, embryos with Renaissance. (B) Expression of S32 in phloem cells and vascular stem cells in the root tip. Scale bars represent 50 µm (root) or 10 µm (embryo).

Figure S3

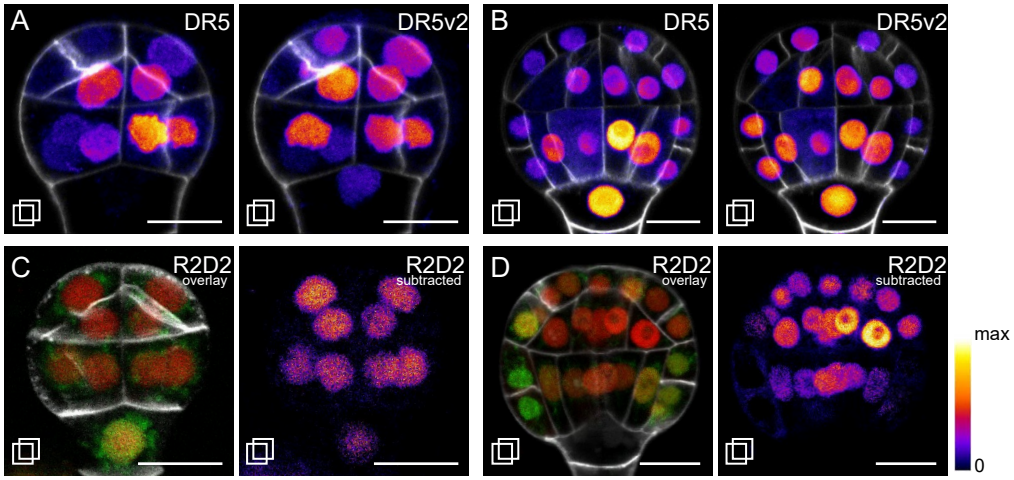

Figure S3: Auxin accumulation and signaling output in the early embryo. 16-cell (A,C) and early globular (B,D) stage embryos reporting the relative amount of auxin or auxin signaling per cell. (A,B) Relative amount of auxin signaling per cell output as reported by pDR5-n3GFP (left) or pDR5v2-ntdTomato (right). (C,D) Relative accumulation of auxin per cell as reported by R2D2. Left: overlay of signals from undegradable pRPS5A-mDII-tdTomato (red), degradable pRPS5A-DII-3xVenus (green) and Renaissance (white). Right: difference between DII signal and mDII signal per pixel. All images are stacks and all scale bars represent 10 µm. □ Indicates images result from a stack.

Figure S4

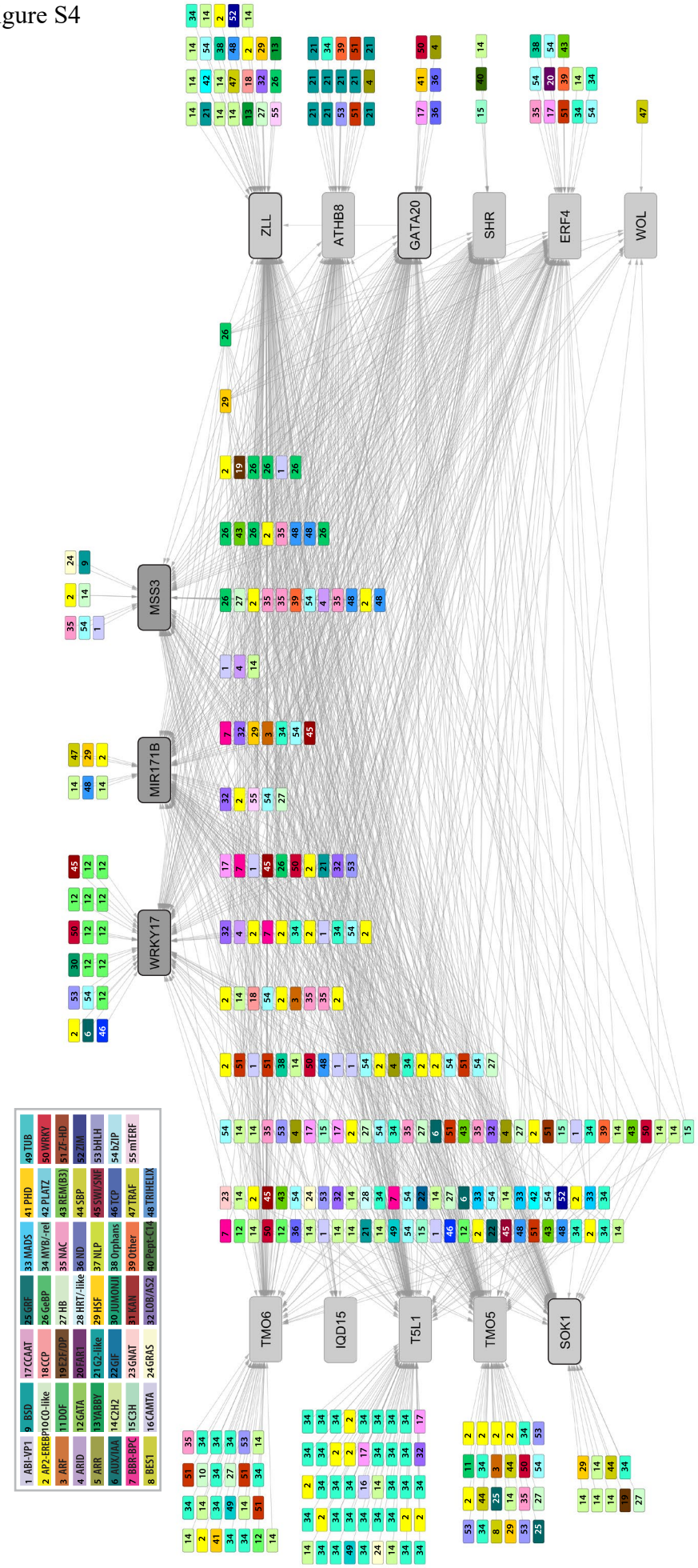

Figure S4: Vascular Yeast One Hybrid network. Network containing all interactors of the 16 vascular promoters screened. Nodes corresponding to promoters are larger and colored grey (dark grey for inverse markers), nodes corresponding to transcription factors (TFs) are placed together based on their outdegree. TF nodes with an outdegree of 1 are placed on the periphery near their target, TF nodes with an outdegree of 2 or higher are placed in the center and are grouped based on their outdegree, nodes with a higher outdegree are located further to the right. Network overview with TF nodes colored according to TF family. Each TF family is represented by a color and number (see insert table).

Figure S5

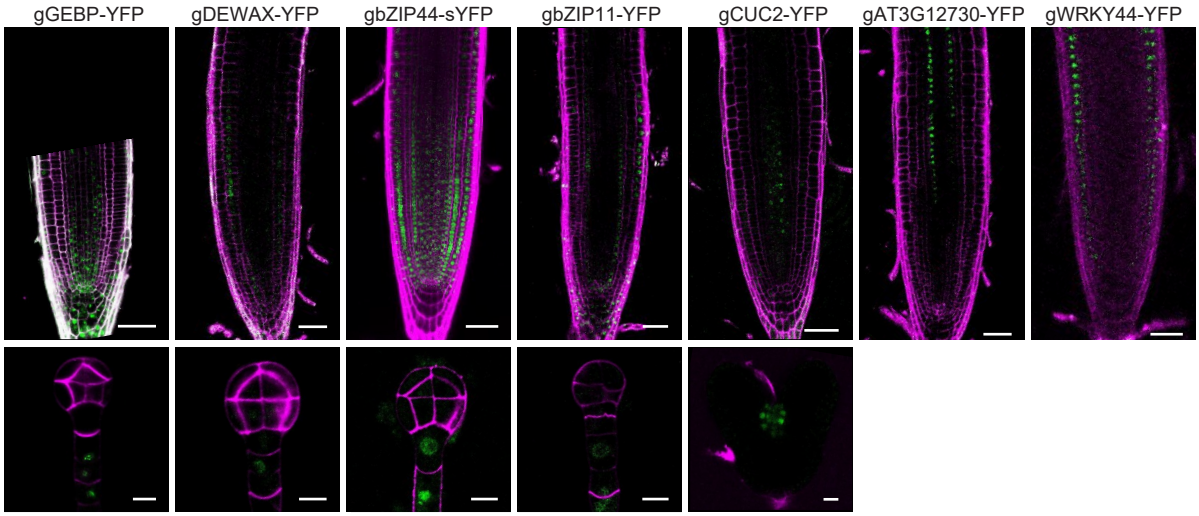

Figure S5: Protein localization of the candidate regulators in root and embryo. In each panel, YFP fusion protein localization in the root is shown at the top, followed by localization in one embryonic stage. Scale bar indicates 50 μm in roots or 10 μm in embryos.

Figure S6

Figure S6: Phenotypes of SRDX-tagged candidate regulator misexpression. (A-D) Adult plants expressing SRDX-tagged candidate regulators under the RPS5A promoter show altered leaf morphology or decreased fertility. (E) No vascular abnormalities are detected in root tip and cotyledon of 5 day old seedlings expressing SRDX-tagged candidate regulators under the RPS5A promoter (n=10). Top and middle panels show longitudinal sections and cross-section of vascular bundles of representative root tips. Nuclear signal is pTMO5::tdTomato. Bottom panel shows the vascular bundles in cleared cotyledons. Scale bars represent 100, 25 and 500 μm in top, middle and bottom panels.

Figure S7

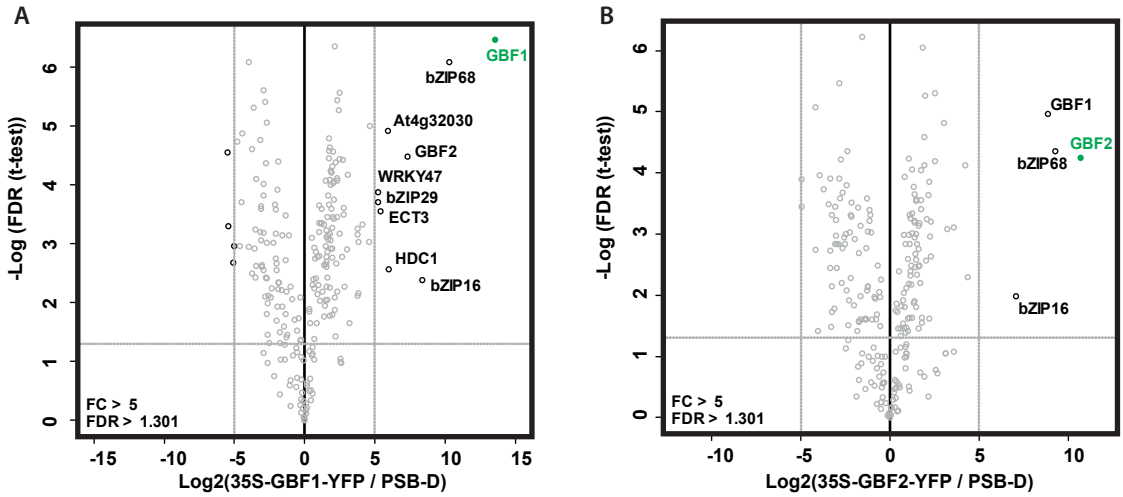

Figure S7: IP-MS/MS experiments confirm that GBF1 and GBF2 can heterodimerize with G-class bZIPs. Results of immunoprecipitation followed by tandem MS (IP-MS/MS) on Arabidopsis cell cultures expressing GBF1-YFP (left) or GBF2-YFP (right) under the 35S promoter compared to wildtype (PSB-D) cell cultures. Volcano plots show fold change (FC, x-axis) and significance (FDR, y-axis) of each detected protein. Proteins with a p-value below 0.05 (-log(FDR)>1.301) and a fold change above 5 are marked and have their name displayed.

Figure S8

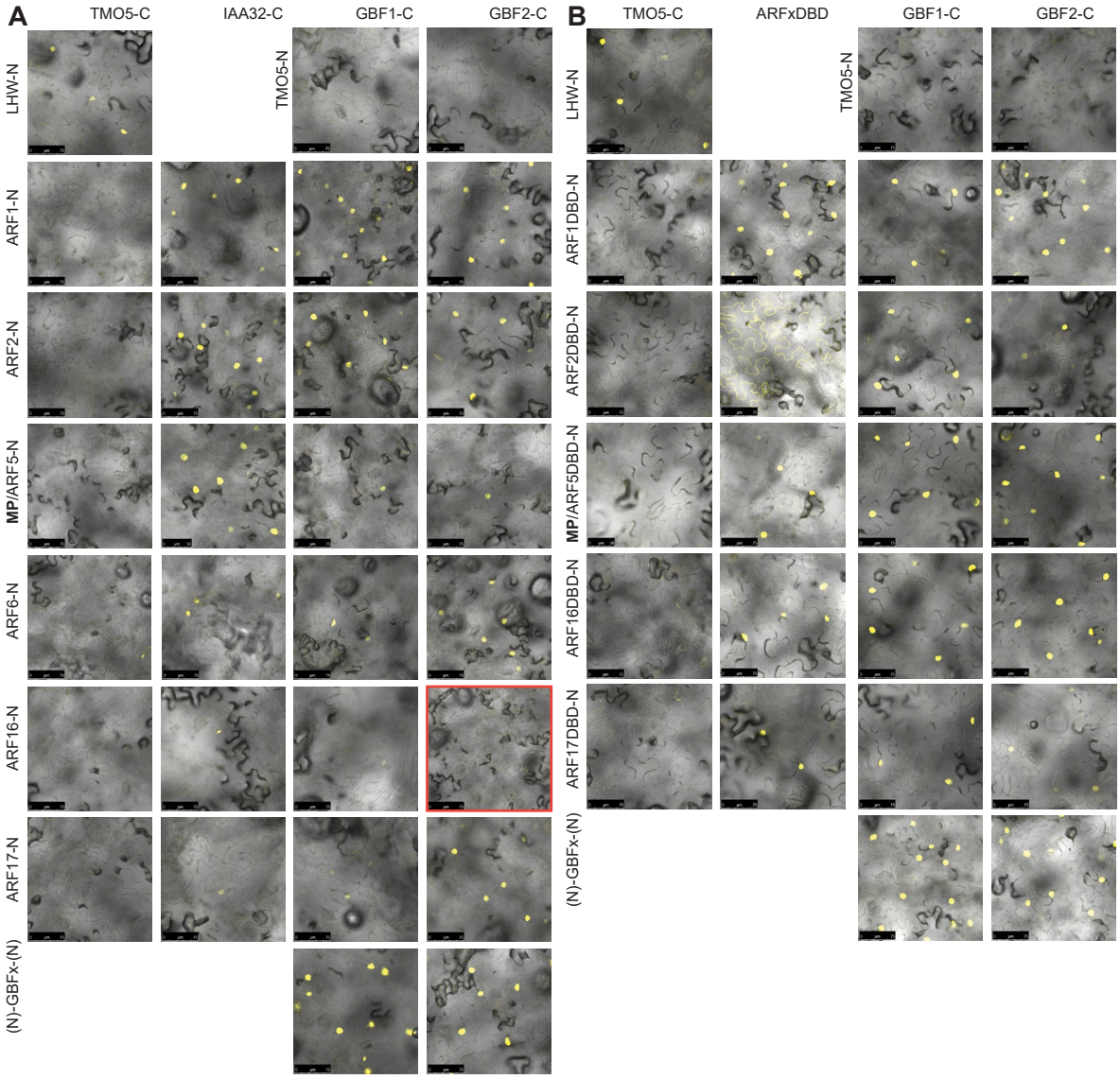

Figure S8: Split-YFP experiments performed using tobacco leaves to confirm GBF-ARF interactions. (A) Interactions GBF1/2-CtYFP and ARF-NtYFP. TMO5 was used as a negative control, homodimerization was used as a positive control for GBF and IAA33 was used as a positive control for ARFs. (B) Interactions GBF1/2-CtYFP and ARFxDBD-NtYFP. TMO5 was used as a negative control and homodimerization was used as a positive control for GBF and for ARFs. LHW was used as a positive control for TMO5. The red square highlights lack of signal.

Figure S9

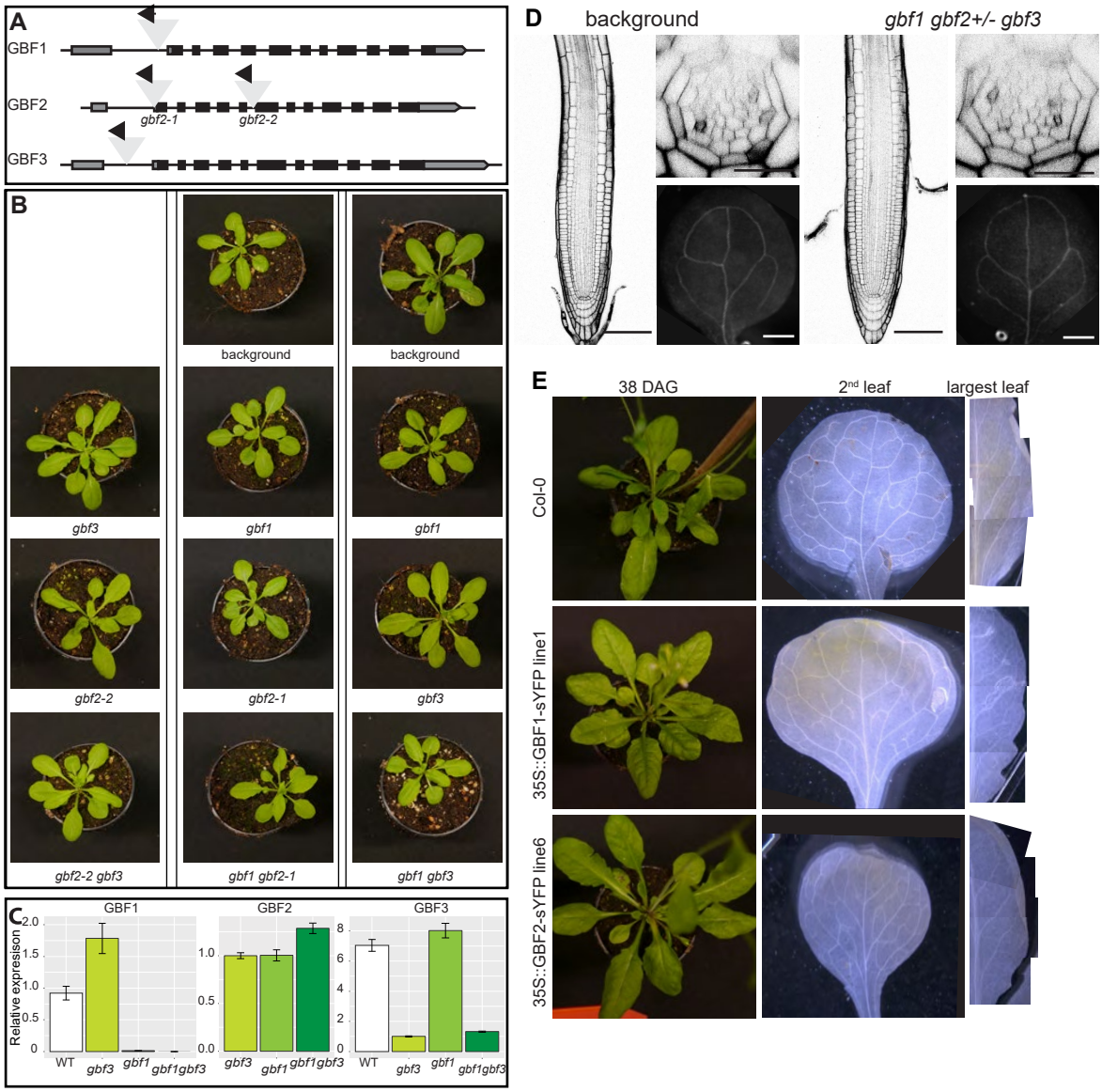

Figure S9: Genetic analysis of GBF function (A) Insert locations of the T-DNA lines used. (B) 24-day old plants of 3 sets of GBF double mutants, single mutants and background plants. (C) Relative expression levels of GBF1, GBF2 and GBF3 in the gbf1gbf3 double mutant and single mutants. (D) No vascular abnormalities are detected in root tip and cotyledon of 5 day old *gbf1 gbf2+/1 gbf3* seedlings (n=12). Top and middle panels show longitudinal sections and cross-section of vascular bundles of representative root tips. Bottom panel shows the vascular bundles in cleared cotyledons. Scale bars represent 100, 25 and 500 µm in top, middle and bottom panels. (E) 35S-GBF1/2 and Col-0 plants 38 DAG. GBF1/2 overexpression lines have early leaves with an increased width/length ratio, late leaves with increased serration and more pronounced veins, and slower development resulting in delayed flowering. No obvious changes in venation pattern were observed.

Dataset S1

Click here to Download Dataset S1

Table S1: List of the full TF collection available in the Brady lab in July 2016.

Click here to Download Table S1

Table S2-: IP-MS/MS performed on MP-GFP indicates MP interacts with GBF2

RATIO	p-value	AGI	Gene names			
254.643933	0.123742533	At2g34440	AGL29			>100 fold cha
227.010877	1.02778E-07	At5g49400	zinc knuckle (CCHC-type) family protein			>50 fold chan
92.7562822	0.034458788	At4g01120	GBF2, bZIP (basic leucine zipper) transcription factor			>20 fold chan
67.3715698	7.58892E-06	At1g19850	ARF5			
35.8005748	0.030648555	At5g15230	GASA4, Gibberellin-regulated protein 4			
34.0032165	0.003322538	AT1G48620	HON5			
25.9888263	0.449902079	At4g08150	KNAT1, Homeobox protein knotted-1-like 1			p-value < 0.05
21.4465118	0.151449903	At2g36930	C2H2-type zinc finger-containing protein			
20.0779792	0.003924551	At5g62690	TUBB2			

Table S3: Ranking of and scores awarded to the 50 initially selected transcription factors.

Left to right: (grey) Final results of the 4 scoring totals and average total ranking. (yellow/pink) Scores awarded based on binding pattern. Includes data on outdegree and binding pattern from the network and DAPseq data from O'Mally. (grey/blue) Scores awarded based on embryo expression. Includes expression percentile data on embryo expression levels of whole WT embryos (Weijers lab) and fold changes from the embryo expression atlas (Palovaara). (green) Scores awarded based on vascular expression. Includes expression fold changes from leaf disk (Kondo) and expression percentile data from root transcriptome atlas (Brady)(Phloem, Stele, Xylem). * HTA2 and ESE3 were excluded.

Click here to Download Table S3

Table S4: P-values resulting from Tukey's tests performed on promoter deletion and protoplast assays.

pGATA20-n3GFP promoter deletions			
	difference	pvalue	signif.
GATA20full - GATA20X12	152.4339	0.0036	**
GATA20full - GATA20X1a	87.2084	0.0817	.
GATA20X12 - GATA20X1a	-65.2255	0.1258	
pTMO5-n3GFP promoter deletions			
	difference	pvalue	signif.
TMO5full - TMO5X12	51.20487	0.0036	**
TMO5full - TMO5X1a	2.669164	0.9792	
TMO5X12 - TMO5X1a	-48.5357	0.0036	**
pGATA20-n3GFP protoplasts			
	difference	pvalue	signif.
empty - G2	-9.25539	0.6488	
empty - Md	45.81004	0	***
empty - MdG2	56.19519	0	***
G2 - Md	55.06543	0	***
G2 - MdG2	65.45058	0	***
Md - MdG2	10.38515	0.5628	
pTMO5-n3GFP protoplasts			
	difference	pvalue	signif.
empty - G2	0.3688	0.9999	
empty - Md	-28.2326	0.0001	***
empty - MdG2	1.452391	0.9944	
G2 - Md	-28.6014	0	***
G2 - MdG2	1.083591	0.9953	
Md - MdG2	29.68504	0	***
pWRKY17-n3GFP protoplasts			
	difference	pvalue	signif.
empty - G2	5.074664	0.6685	
empty - Md	16.31392	0.0019	**
empty - MdG2	-5.34845	0.6253	
G2 - Md	11.23925	0.0543	.
G2 - MdG2	-10.4231	0.0855	.
Md - MdG2	-21.6624	0	***

Table S5: Primers used in this study

Gene Name	Locus		Sequence	Promoter length (kb)
MIR171B	AT1G11735	sense	ACGGCAAAAAAGACGTCACC	2.0
		antisense	taaaaccactcttgttcgac	
GATA20	AT2G18380	sense	taccaatccgatcttgatcc	3.0
		antisense	gaaattgaagactacagatagag	
MSS3	AT2G43290	sense	catggtacatcagaatgtataacc	3.0
		antisense	aactgttgaatcacaactc	
ERF4	AT3G15210	sense	ATCAACTTTATGTGCAGCAGC	3.0
		antisense	tctcggatagatagattagag	
MEE45	AT4G00260	sense	gtgcaattctatagctttcttgg	3.0
		antisense	tttcaaaatcttgagaagtcc	
AP2B3	AT4G03170	sense	CAACCAAAATCCTTGATAATGTC	1.5
		antisense	gatcgatctctcacgttctc	
SOK1	AT1G05577	sense	CGTTCCGTGGTGAATCAATG	2
		antisense	CTCTCTTTCTTTTTGTTTTGGTCT	
MIR171B	AT1G11735	sense	acggcaaaaaagacgtcacc	2
		antisense	taaaaccactcttgttcgac	
T5L1	AT1G68810	sense	acggaaaattgtggatttg	1.2
		antisense	aaggaaaggttggtaaaagaagg	
WOL	AT2G01830	sense	ccgttttatcttcctctacaaaaatcc	2
		antisense	cacttcaaatgtaggtattcc	
GATA20	AT2G18380	sense	taccaatccgatcttgatcc	3
		antisense	gaaattgaagactacagatagag	
WRKY17	AT2G24570	sense	caataatttatctcgtggagg	3
		antisense	gatgagaaaccagaggag	
PEAR1	AT2G37590	sense	ccaccatcgataatcgaatgacc	1.3
		antisense	ggttattctcttttgattttattcttc	
MSS3	AT2G43290	sense	catggtacatcagaatgtataacc	3
		antisense	aactgttgaatcacaactc	
ERF4	AT3G15210	sense	ATCAACTTTATGTGCAGCAGC	3
		antisense	tctcggatagatagattagag	
TMO5	AT3G25710	sense	tgattttcacaatttaagggtcgg	2.9
		antisense	tttttggttttttggttttttagtttttggg	
DOF6	AT3G45610	sense	tctgcggatcctcaatcac	
		antisense	tctcaaccaattgagaaac	
IQD15	AT3G49380	sense	ccggagatcttaaaattatatagc	1.4
		antisense	caagatcgatcaacctcgtctgc	
ATHB8	AT4G32880	sense	ctttgatcctctccgatctctc	1.2
		antisense	cctgctgccacatacacattgg	
SHR	AT4G37650	sense	agaagcagagcgtggggtttc	2.5
		antisense	ttttaatgaataagaaaatg	
ZLL	AT5G43810	sense	AGGCCGGTGGTTTGCATATC	2.9
		antisense	TTTTTGTTGTTTGGATTTTCAAAAACTC	
TMO6	AT5G60200	sense	gcattaggtcgaatagg	
		antisense	aagagctgaatctgag	
AT3G53680	AT3G53680	sense	agaagatgatgagagtgaagc	2.8
		antisense	TCCCTGATACTCTCGGCTTGTAGC	
BPC4	AT2G21240	sense	ctaggaaacctgttccaatacc	3
		antisense	CTTGATAGTGATGTAGCGGTTTGTC	
GLP3	AT2G36340	sense	gatatataccaacactgtatatgacc	3
		antisense	AGGAGAAACTCCTAAGTTTGC	
STKL2	AT4G00250	sense	AGAGTCGTTAACCACTTCACACC	3
		antisense	GTTGGTTTGAGCAAGCACC	
GBF1	AT4G36730	sense	CTATAAAGTCGGAGATGATGG	3
		antisense	ATTTGTTCCTTCACCATCTTTCG	
GBF2	AT4G01120	sense	gatcattctatacatgcatcg	3
		antisense	GCTAGCCGCGACAGGATCGGTTATCG	
STKL1	AT4G00238	sense	CAATCGATTCAAACTCTGTGAAAGG	3
		antisense	GTTGGTTTGAGTAAGCACTGAAGTC	
AT4G03250	AT4G03250	sense	GTATACAAAGATGTGAAGAGAGG	3
		antisense	ATCCATTGACGAGCTAGATTCG	
ASIL1	AT1G54060	sense	cagctgtgactttagctaaagg	3
		antisense	GCTACTTACATTGCCGTTATTCTTGC	
REM35	AT4G31615	sense	gaccaggtactttatgtttgc	3
		antisense	TTGACCTGACTTGAGCATGTAAGG	

BiFC			
GBF1		sense	ctagttggaataggttCATGGGAACGAGCGAAGACAAGATGC
		antisense	tatggagttgggttaattaATTTGTTCCTTCACCATCTTTCG
GBF2		sense	ctagttggaataggttCATGGGTAGCAACGAAGAAGG
		antisense	tatggagttgggttaatcaGCTAGCCGCGACAGGATCG
TMO5		sense	TAGTTGGAATAGGTTCATGTACGCAATGAAAGA
		antisense	GTATGGAGTTGGGTTCATTATAACATCGATTCACCATC
LHW		sense	TAGTTGGAATAGGTTCATGGGAGTTTTACTAAGAGA
		antisense	GTATGGAGTTGGGTTCCATTGAACAGCCACCAGTAACC
ARF1		sense	TAGTTGGAATAGGTTCATGGCAGCTTCCAATCATTCATCT
		antisense	AGTATGGAGTTGGGTTCTCATCTTGATCCCGCCATAG
		DBDanti	AGTATGGAGTTGGGTTCaggaccagatggaccagtggc
ARF2		sense	TAGTTGGAATAGGTTCATGGCGAGTTCGGAGGTTTC
		antisense	AGTATGGAGTTGGGTTCTTAAGAGTTCCCAGCGCTGGACA
		DBDanti	AGTATGGAGTTGGGTTCAACAGGACTCAAAGCAGGAGG
ARF5		sense	TAGTTGGAATAGGTTCATGATGGCTTCATTGTCTTG
		antisense	agtatggagttgggttcTGAAACAGAAGTCTTAAGATC
		DBDanti	AGTATGGAGTTGGGTTCgctaccccattcagtttcacc
ARF6		sense	TAGTTGGAATAGGTTCATGAGATTATCTTCAGCTGG
		antisense	agtatggagttgggttcGTAGTTGAATGAACCCCCAAC
		DBDanti	AGTATGGAGTTGGGTTCAAGGCCATGGAAAGATGGGAG
ARF16		sense	TAGTTGGAATAGGTTCATGATAAATGTGATGAATCC
		antisense	AGTATGGAGTTGGGTTCTTATACTACAACGCTCTCAC
		DBDanti	AGTATGGAGTTGGGTTCgatcagattgttgtaatctg
ARF17		sense	TAGTTGGAATAGGTTCATGTCACCGCCGTCGGCAAC
		antisense	AGTATGGAGTTGGGTTCTTAACCTTGGGAGCTAGAAC
		DBDanti	AGTATGGAGTTGGGTTCtccactcaagaaccctcctcc
Genotyping			
pRPS5A-GAL4			
insertion site		sense	CACGGGTAAACGGCCAACGGATTCACC
		antisense	ctccaccacccccaattcgaccgagc
GAL4			GCAAACCAGCGTGGACCGCT
SALK LB			ATTTTGCCGATTTCGGAAC
SALK_027691		WT LB	TATTATGTTCAGCAGTCCCGG
		WT RB	TTCGTTGAGTGTTGGTTTCTG
SALK_206654		WT LB	TTGGTGATCTTTGTTGCCTTC
		WT RB	TGGTGGAGTTTATGCTCATCC
SALK_205706		WT LB	TGGATATGGTGCTCCATAAGG
		WT RB	CGCTCTGTTTTCTCGAGAAAG
SALK_067963		WT LB	ATAGCTGCCCAATCAGGGTAG
		WT RB	CTTCAAGGAGCTTTCGGATTC
ChIP qPCR			
WRKY17 box		sense	ATTAGATCGAGCTGCAAATTG
		antisense	TTTACCACGGCAACTGAT
WRKY17 control		sense	GAGGTTACATTGACTTCT
		antisense	ATTAGTTAGTGGATGATAGA
GATA20 box		sense	TTGGTAATCTAAGAGAGA
		antisense	ATAAGTGTTGTGTATCTG
GATA20 control		sense	TACCAATCCGATCTTGAT
		antisense	TGATTAACTCGCATCTTG
TMO5 box		sense	GGTTTGGCTATACGAAAC
		antisense	AGAATTTCATTTGGCTGC
TMO5 control		sense	CACAATTTAAGGGTCGGAAA
		antisense	AATATAATTGACTCCACCATGT
ERF4 box2		sense	GCCAATTAACAACCAAAT
		antisense	AGAATGGATGAAGAGAGA
ERF4 box1		sense	AAAGATAAGTGGAGGTAA
		antisense	TGTGATAGATAATTGAAGG
ERF4 control		sense	ACACCACCCGTTGAGAAT
		antisense	TTGAATTTGCGGAAACTTTGTT

Cloning promoter deletions		
WRKY17_full	sense	TAGTTGGAATGGGTTCGAACaataatttatctcgtggagg
	antisense	TTATGGAGTTGGGTTCGAAgatgagaaaccagaggag
WRKY17_reg1	sense	cttcaactcaatctcagccgtaagcaccgatttgactaaactcc
	antisense	ggagtttagtcaaatcggtgcttacggctgagattgagttgaag
WRKY17_reg2	sense	gacaatttatgagtcagccagaattagatcagttgccgtggtaaaagg
	antisense	ccttttaccacggcaactgatctaattctggctgactcataaattgtc
TMO5_full	sense	TAGTTGGAATGGGTTCGAAtgattttcacaatttaagggtcgg
	antisense	TTATGGAGTTGGGTTCGAAtttttggttttttggttttttagtttttggg
TMO5_reg1	sense	gattaaaagtaaaagtctttttgggtcagtgtttgtttttattc
	antisense	gaataaaaaacaaacactgacccaaaaagacttttacttttaatc
TMO5_reg1a	sense	GTCTCTGGTCGGTCGACAGGTCAGTGTTTGTTTTTTATTC
	antisense	GAATAAAAAACAAACACTGACCTGTCGACCGACCAGAGAC
GATA20_full	sense	TAGTTGGAATGGGTTCGAAtaccaatccgatcttgatcc
	antisense	TTATGGAGTTGGGTTCGAAgaaattgaagactacagatagag
GATA20_reg1	sense	gtcgttacttaagtttccacagtttgtaacttgtaac
	antisense	gttacaagttacaaactgtggaaacttaagtaacgac
GATA20_reg2	sense	gtgaaaggagcttggtaatctaagaaaaactgcagatacacaacac
	antisense	gtgttgtgtatctgcagtttttcttagattaccaagctcctttcac
GATA20_reg2a	sense	CCTTAGAAAACCGTGACATTGTCACGCCTCTTTTGACCAACCCCG
	antisense	CGGGGTTGGTCAAAAGAGGCGTGACAATGTCACGGTTTTCTAAGG
ERF4_full	sense	TAGTTGGAATGGGTTCGAAATCAACTTTATGTGCAGCAGC
	antisense	TTATGGAGTTGGGTTCGAAtctcggatagatagattagag
ERF4_reg1	sense	caaaattctttgaaagaggaaagaaaagataagtggaggtaaaaaag
	antisense	ctttttacctccacttatctttttcttcctctttcaaagaattttg
ERF4_reg2	sense	ccattctccacgcgtcgcgactatacatctttaaaactc
	antisense	gagttttaaagatgtatagtcgcgacgcgtggagaatgg